

# Statistical Characterization VBR MPEG at the Slice Layer

M. R. Izquierdo  
D. R. Reeves

Center for Communications and Signal Processing  
Department of Electrical and Computer Engineering  
North Carolina State University

TR-94/17  
July 1994

# Statistical Characterization VBR MPEG at the Slice Layer

Michael R. Izquierdo  
mikeiz@vnet.ibm.com  
(919) 543-0104

Douglas R. Reeves  
reeves@eos.ncsu.edu  
(919) 515-2044

Department of Electrical and Computer Engineering  
North Carolina State University  
Raleigh, North Carolina 27695  
fax: (919) 543-6552

July 29, 1994

## Abstract

We studied the ATM cell-generation statistics of three VBR encoded MPEG video sequences at the Slice layer. Each of the video sequences contained Intracoded (I), Predictive-coded (P) and Bidirectional-coded (B) frames and included special camera effects such as zooming, panning and sudden scene changes. Each sequence consists of 150 frames at a rate of 30 fps. Previous research characterized sequences which did not include B frames. This was due to its long encode time making it unattractive for real-time video applications. We examined video sequences with B frames since they offer the highest amount of compression and increased bit-rate variation which can be exploited when multiplexing multiple video streams. Also, it is likely that applications where video is stored for retrieval will contain B frames. The motivation behind studying the cell generation process at the Slice layer is that the slice size makes it well suited for transport packet payloads. It would be feasible to have ATM Convergence Sublayer (CS) payloads consisting of slices where destination nodes can detect slice errors and provide corrective action or attempt error concealment. Also, characterization at the Slice layer captures the spatial behavior of each frame.

We calculated quantitative metrics such as compression ratio and picture density to compare the video sequences and discuss the effects of content on these metrics. We determined that the compression ratio can differ by a factor of 5 due to content. We showed the macroblock type distribution for each sequence based on frame type and discussed their effects on compression ratio. We gave the distribution of cells/slice for each sequence and determine if the gamma distribution is a good fit by using QQ plots. We found that none one of the sequences fits the gamma distribution well. This makes it unlikely that a single distribution can apply to all I/B/P video streams. We noted that, at the Slice layer, the data is highly correlated with negative linear decay. Also, peak-to-mean ratios varied from 3.9 to 6.2 and the coefficients-of-variation varied from .97 to 1.09. We pointed out that dynamic bandwidth allocation schemes which request bandwidth in fixed symmetric increments might not be appropriate for sources with I/B/P frames. We presented a multiplexing scheme whereby video streams are time shifted in order to overlap B frames from one stream with I and P frames of another. We found that the peak-to-mean ratio and coefficient-of-variation is reduced and that the multiplexed output stream fits the Gamma distribution well. Finally, we used the Markov Chain to model the cell generation process and show that an 8 state Markov Chain is able to match the cells/slice distribution well.

## 1.0 Introduction

The Asynchronous Transfer Mode (ATM) Network has gained much attention as an effective means to transfer voice, video and data information over computer networks. The use of a fixed size, fifty-three byte cells to transfer data makes ATM well suited to support isochronous type services like voice and video [1]. The small cell size makes it possible to interleave cells from other sources over a common communications link, thereby providing low end-to-end latency. The transport of video data over ATM networks has been a fertile area of study. Specifically, much work has been done in the area of the transport of compressed video over ATM, addressing such issues like bandwidth allocation, modeling, multiplexing, encoding methods (CBR vs. VBR), QoS<sup>1</sup>, etc. We attempt to address some of these issues in this paper by investigating the transport of MPEG-1 VBR encoded video over ATM.

We define a method of transporting video using ATM AAL-5 where Convergence Sub-layer (CS) packets are built from MPEG-1 Slices. In this paper, we use an MPEG-1 Video Packet Elementary Stream (VPES) which does not contain audio. In order to understand the impact this data stream will have on the ATM network, we statistically characterized three MPEG-1 encoded video sequences at the Slice Layer. The majority of work has dealt mainly with characterizing video at the Frame Layer which is a natural encoding boundary. However, we believe that error recovery and possibly forward error correction (FEC) are best done at the Slice Layer rather than the Frame Layer. We chose the Slice Layer because it is the lowest independent data unit in MPEG and does not require any data from any other Slice within a Frame for decoding. This makes it possible to provide error-detection, correction or concealment on a portion of a Frame rather than the whole Frame.

We use a model of a video server, shown in Figure 1, which sends ATM AAL-5 type CS packets over an ATM network to a video client. The video server parses the video stream in accordance to the MPEG-1 syntax and builds AAL-5 CS packets from MPEG Slices. Non-Slice data, such as Sequence Layer headers, are placed in its own CS packet. AAL-5 packets are segmented into 53 byte cells with each cell consisting of 48 bytes of video data payload. Cells are transported over the ATM network to a video client which reassembles the CS packet and checks for any errors. The error recovery mechanism would be contained in the video client. One possible example of an error recovery mechanism would be a Reed-Solomon FEC scheme where a CS packet could be corrected when a cell was either dropped or corrupted by the network. We focus our attention on the video server cell

---

1. QoS stands for Quality of Service

stream output into the ATM network. We assumed zero delay between the generation of CS packets, since the assumption was that video data was immediately accessible from a local file system located on storage media.

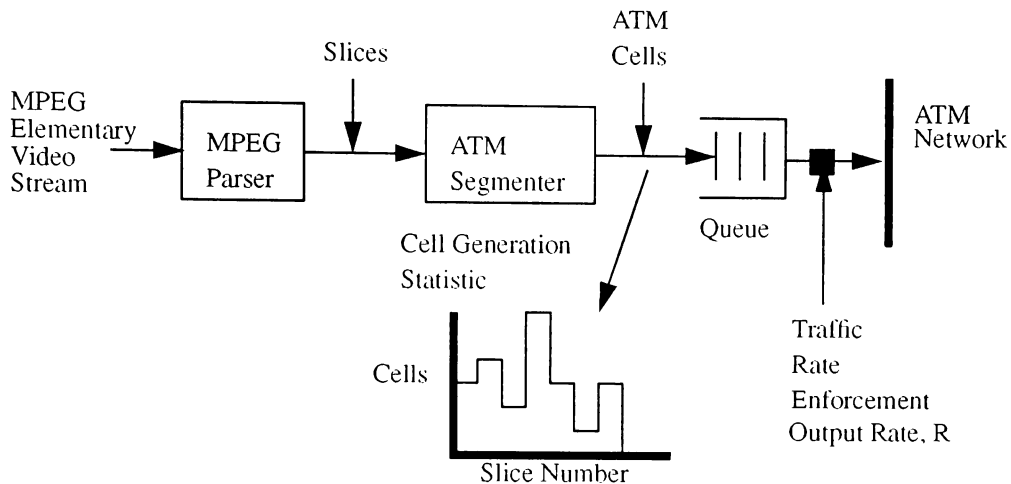


**FIGURE 1. VBR video server model to analyze cell generation statistic**

We studied three video sequences, obtained from the Stanford University FTP<sup>1</sup> archive, called *Bike*, *Flowg* and *Tennis*. We used the software decoder from the University of California at Berkeley called *mpeg\_play* to view the video sequences and study their content. Each video sequence was VBR encoded with a quantization scale ( $q$ ) triplet of (4,4,8). This means that  $q$  was set to 4 for I and P anchor frames and 8 for B reference frames. The video sequences were considered to be high quality encoded. All sequences contained 150 frames and had an Interframe-to-Intraframe ratio ( $M$ ) equal to 2. We developed a program, written in C, which parses an MPEG-1 stream and extracts Slice and Frame data. The program also extracts and decodes all Sequence, Frame and Slice header information. Matlab 4.0 was then used to analyze the Cells/Slice data.

We calculate metrics such as the mean picture density and compression ratio to gain an understanding of the effectiveness of MPEG-1 encoding on different scene content and how they relate to the statistics. This was possible because each sequence was encoded using the same quantization values. We calculate statistics such as peak-to-mean ratio (PMR), coefficient-of-variation (CV) and autocorrelation in order to understand the

1. FTP is the File Transfer Protocol used in TCP/IP.

amount and behavior of the variability in the data. We compare the probability mass function (pmf) of each of the video sequences to the Gamma distribution by using the QQ plot. Recent papers have shown that MPEG sequences with only I/P frames fit the Gamma distribution well. We try to determine if this is also true for video sequences with I/B/P frames.

We introduce a multiplexing scheme, for VBR video with I/B/P frames, which we call *Time-Shifted Multiplexing* (TSM) which attempts to take advantage of the periodicity we found in I/B/P video sequences. We show a model of each of the sequences based on an 8-state discrete-time, discrete-state Markov Chain where each state represents a range of Cells/Slice values. The number of states was chosen to be approximately equal to the number of standard deviations between the peak and the minimum number of Cells/Slice. Finally, we discuss the impact of I/B/P sequences on dynamic bandwidth allocation schemes

## 1.1 VBR vs. CBR

There are two basic methods to encode video: variable bit-rate (VBR) and constant bit-rate (CBR). VBR encoders attempt to keep the video quality constant by not changing the quantization scale in order to maintain constant bit rate output. VBR encoded video trade-off constant bit-rate output for constant video quality. This variation in output bit-rate presents more of a challenge for computer networks in terms of bandwidth allocation and guarantees for QoS such as cell loss. The CBR encoding technique attempts to remove the variability of the video stream by varying the picture quality. This scheme requires a rate-control buffer at the output of the encoder, shown in Figure 2, where the quantization level is changed when the rate control buffer approaches an underflow or overflow condition. As the buffer approaches an overflow condition, the bit-rate is reduced by increasing the quantization level. When an underflow condition is detected, the bit-rate is increased by decreasing the quantization level. This variation in video quality is an undesirable effect of encoding video using the CBR method. However, transmitting video using CBR makes it easier to request bandwidth when establishing an ATM connection.

VBR encoding has several advantages over CBR which have been pointed out in previous work such as: (1) constant and subjectively better video quality, (2) simpler encoder design, (3) increased gain when multiplexing multiple sources. VBR not only produces a constant quality level, but also a subjectively better video quality level. Morrison [2] compared the luminance Signal-to-Noise (SNR)<sup>1</sup> ratio of CBR and 1-layer VBR and showed significant reductions in SNR of up to 7 dB. Another advantage to using VBR is the gain

achieved by statistically multiplexing multiple VBR sources. Verbiest, et al. [3] has shown that the statistical multiplexing of multiple VBR sources provides a gain of a factor of two over multiple CBR sources.

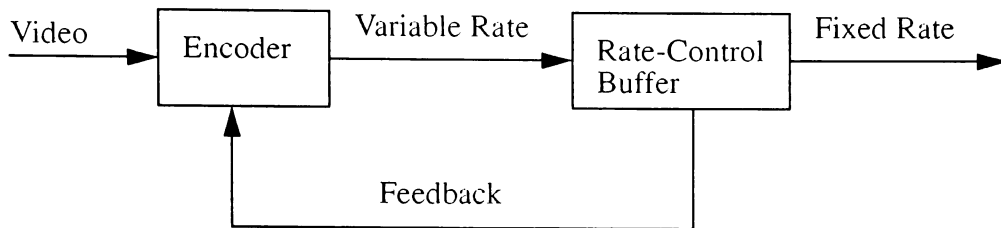


FIGURE 1. Basic CBR coding scheme

## 1.2 VBR Video Transport

One of the main drawbacks of transmitting compressed video using VBR is that the probability of cell-loss can increase when transporting cells over ATM networks. This is caused by the variability in the cell stream where the source exceeds the allocated bandwidth. The user must specify its bandwidth requirements when establishing a connection in order for the network to determine if enough resources exist. This method is a preventative congestion control technique in that flow control is done at the source prior to congestion [4]. The user can specify a bandwidth allocation at the peak rate; however, this would not be an efficient utilization of bandwidth.

Dropping cells from the video stream without regard to content can cause serious degradations in picture quality. MPEG-1 was developed to operate over lossless connections and does not define a transport protocol<sup>1</sup> to deliver compressed video data over networks. As a result, several techniques have been developed to either reduce the effects of cell-loss with VBR video sources or minimize the amount cell-loss.

### 1.2.1 Two Layer Codecs

A two-layer codec is used to reduce the effects of cell-loss by dividing the encoder output into two streams [5], [6]. The first stream is produced by the Base Layer and is a CBR

---

1. SNR is used as a measure of video quality and is computed as the mean square error between the input pixels to the encoder and the decoded output.

1. This has recently changed with the announcement of the MPEG-2 draft standard which defines Transport Layer for lossy connections.

stream consisting of high priority cells transported over a lossless, or high quality, connection. The second stream is produced by the Enhancement Layer and is a VBR stream consisting of low priority cells transported over a lossy connection. The Base Layer contains the basic structural information of the picture while the Enhancement Layer contains the difference between the input stream and the decoded output of the Base Layer. When traffic exceeds the allocated bandwidth, the network will drop low priority cells from the Enhancement Layer in order to prevent network congestion. Both streams are combined at the decoder in order to reproduce the video stream.

The two-layer codec makes the video stream more resilient to cell-loss. Morrison [2] indicated that a one-layer codec must operate with cell losses not greater than  $10^{-5}$  before a degradation of quality is visible. However, for two-layer codecs it is possible to operate with cell loss rates at  $10^{-3}$ . Kishino, et. al. [7] compared one-layer encoded pictures, where cells were dropped at random, to pictures which were two-layer encoded and low priority cells were dropped. The results showed that the quality of the one-layer encoded picture with random cell-loss at a rate of 5% was significantly worse than a two-layer encoded picture with 50% loss of low priority cells.

### 1.3 Dynamic Bandwidth Allocation

Another technique, called Dynamic Bandwidth allocation, tries to prevent cell-loss by changing the allocated bandwidth during a connection by predicting that additional bandwidth will be required in the near future based on the recent behavior of the traffic stream. This scheme requires a fast-reservation protocol (FRP) [8] to reserve extra bandwidth upon request. The unit which monitors the traffic and requests additional bandwidth is referred to as the Traffic Predictor. One example of this technique was proposed by Pancha, et. al. [9] which allocates bandwidth at the mean rate when a connection is established and increases or decreases bandwidth by one standard deviation based upon the bit-rate behavior of the source. This requires full statistical characterization of the video stream in order to calculate the mean and standard deviation. A Markov-chain was used to show that the probability of the bandwidth changing by more than one standard deviation was negligible. We will show that while this is true for sequences containing I/P frames is not the case with sequences containing I/B/P frames.

Another example is found in Heeke [10], where sources are divided into multiple rate classes with each class transferring data at a different rate. Having a finite number of rate classes limits the number of transmission rates which makes the modelling of the video traffic simpler. The model consists of a discrete-state, continuous-time Markov Chain

where each state represents a rate class. Traffic is monitored by a video control unit which uses a unique policing algorithm to ensure the traffic does not exceed the bit-rate of the rate class. If this occurs, the video control unit can temporarily switch the video traffic to a higher rate class. One can see a similarity between this technique and that proposed by Pancha, et al. in that if the rate classes were separated by one standard deviation then the bit-rate jumps would be equivalent.

## 2.0 MPEG-1 Overview

The MPEG -1 standard was submitted for approval to the ISO-IEC/JTC1 SC29 standards body in November of 1991. The standard was prepared by the SC29/WG11 committee also known as the Motion Picture Experts Group (MPEG). The standard is divided into four parts titled: (1) ISO/IEC 11172-1 Systems, (2) ISO/IEC 11172-2 Video, (3) ISO/IEC 11172-3 Audio and (4) ISO/IEC 11172-4 Conformance Testing. This paper specifically deals with 11172-2 Video [11] part of the standard.

The MPEG compression algorithm is asymmetric in that it takes much more time and compute power to encode video than to decode it. Asymmetric techniques are well suited for situations where video data is compressed off-line and stored for future play-back. The objective is to make the decoders simple and inexpensive. A good overview of MPEG is found in DeGall [12]. In symmetric video compression algorithms, the encode/decode computational burden is balanced which shifts some of the encoder complexity to the decoder. This makes the encoder less expensive and the decoder more expensive. The time it takes to encode video decreases as well.

The standard defines constraints, shown in Table 1, on the format, encoding and decoding parameters of the video stream. A video bit stream which adheres to the constrained parameters is referred to as a Constrained Bit Stream (CPB). The actual syntax of the MPEG bit-stream allows for values greater than the constrained parameters; however, adhering to CPB sets limits on the bandwidth, buffer sizes and memory bandwidth. MPEG videos typically come in two Standard Interface Formats (SIF) dimensions: 352x240 pixels @ 30 fps (330 macroblocks/picture<sup>1</sup> maximum) and 352x288 pixels @ 25fps (396 macroblocks/picture maximum).

---

1. The standard uses the term picture instead of frame in an attempt to distinguish a picture from a frame. Most all publications today use the term frame rather than picture and we attempt to do the same. However, throughout this paper the term picture and frame should be thought of as being synonymous.

Horizontal Picture Size	Less than or equal to 768 pels
Vertical Picture Size	Less than or equal to 576 lines
Max Macroblocks per Picture	Less than or equal to 396 macroblocks
Pel rate	Less than or equal to 2 534 400 pels per second
Picture rate	Less than or equal to 30 pictures per second
Motion vector range	Less than -64 to +63.5 pels (using half-pel vectors) (vector scale code $\leq 4$ )
Input buffer size (in VBV model)	Less than or equal to 327 680 bits
Bit-rate	Less than or equal to 1 856 000 bits/second (constant bit-rate)

**TABLE 1. Summary of Constrained Parameters**

## 2.1 MPEG Compression Technique

MPEG essentially relies on two techniques for compression: block-based motion compensation which takes advantage of temporal redundancy and discrete cosine transform (DCT) which takes advantage of spatial redundancy. There are two types of motion compensation used in MPEG: prediction and interpolation. Prediction assumes that the current picture block can be created from a past or future frame's picture block. Interpolation references picture blocks from both a past and future frame and uses a mathematical combination of the two (usually the average) to create the current picture block. This method is usually computational intensive, but provides the most compression.

### 2.1.1 Spatial Compression

In MPEG, spatial compression is accomplished by using the two-dimensional Discrete Cosine Transform (DCT), quantization and run length coding. Frames which use spatial compression solely are referred to as Intra-coded frames or I frames. The DCT operates on an 8x8 matrix of pel values called a Block. The DCT translates the time domain representation of the Block into the frequency domain and outputs a DC coefficient and a number of AC coefficients. The Inverse Discrete Cosine Transforms (IDCT) converts the block from the frequency domain back to the time domain. The two-dimensional DCT,  $F(u, v)$  and the IDCT,  $f(x, y)$  are shown below.

$$F(u, v) = \frac{1}{4} C(u) C(v) \left( \sum_{x=0}^7 \sum_{y=0}^7 f(x, y) \cos \frac{(2x+1) u \pi}{16} \cos \frac{(2y+1) v \pi}{16} \right)$$

$$f(x, y) = \frac{1}{4} \left( \sum_{u=0}^7 \sum_{v=0}^7 C(u) C(v) F(u, v) \cos \frac{(2x+1) u \pi}{16} \cos \frac{(2y+1) v \pi}{16} \right)$$

$$C(u), C(v) = \frac{1}{\sqrt{2}} \quad \text{for } (u, v) = 0$$

$$C(u), C(v) = 1 \quad \text{otherwise}$$

The value of the coefficient is divided by the quantizer step and rounded to the nearest whole number.

The DC coefficients of the luminance and chrominance blocks are coded using a Differential Pulse Code Modulation technique (DPCM) in which the DC coefficients of the current block are subtracted from the preceding block with the result used. A Variable Length Code<sup>1</sup> (VLC) is then used to represent the absolute value of the result which differ for luminance and chrominance. The DC coefficient of the first macroblock within a Slice is an absolute value which makes Slices independent from each other. One can see that if the first macroblock within a Slice is corrupted, the whole Slice could decode erroneous DC coefficient values. If a macroblock towards the end of a Slice were corrupted only those macroblocks which follow will have their DC coefficients corrupted.

AC coefficients are Run Length Coded (RLC) using a combination of the Run-Length and Level code. The Run-Length value is the number of zero AC coefficients skipped between non-zero coefficients. The non-zero AC coefficients are specified using the Level code. This technique takes advantage of the fact that most of the AC coefficients are zero.

### 2.1.2 Temporal Compression

Temporal compression is accomplished by using a motion compensation technique. Frames which employ motion compensation are referred to as Inter-coded frames. Motion

---

1. Variable Length Codes use fewer bits to represent data which occurs with high frequency and more bits to represent data which occur with low frequency. Since the luminance does not differ greatly between adjacent blocks, the codes for small difference use the fewest bits (2 to 3) while larger differences use up to 7 bits.

compensation achieves video compression by sending a reference pointer or motion vector to a past or future picture block instead of sending the DCT coefficients. In almost all cases, sending a pointer to a past or future picture block requires less bits than sending the actual coefficients. Motion compensation is block based in that a 16x16 pel area of the current picture is used to match against a past or future block. If an exact match is found, only the pointer is sent. If a close match is found then the difference between the two blocks is sent along with the pointer. If an exact match is found with a block in the same position, no pointer is sent and the block is skipped by specifying a skip-indicator. The skip-indicator tells the decoder to use the values of the block contained in the past picture in the current position.

There are basically three types of motion compensation used in MPEG: forward-predictive, backward-predictive and bidirectional-predictive. Forward-Predictive motion compensation tries to match blocks from a past frame, whereas Backward-Predictive tries to match blocks from a future frame. Bidirectional-Predictive motion compensation tries to match blocks from both a past and future picture and then uses an mathematical method (typically the average) in order to synthesize the current block. This technique is referred to as interpolation. Block matching can be exhaustive in that all blocks within a frame are searched; however, typically a specific search area is specified for encoding (e.g. +/- 16 pels or +/- 7 pels).

## 2.2 MPEG Layered Structure

The standard specifies the syntax for compressed video streams and consists of six layers which are listed in Table 2. Each layer is identified within the video stream by a Start Code Prefix followed by a unique Start Code listed in Table 3. All layers, except for the Block<sup>1</sup> Layer, contain header information. The layering approach allows for the efficient parsing of the compressed video bit stream which is required to support random access, forward and reverse picture scanning, picture editing and error recovery.

---

1. The Block Layer should not be confused with a pel block which is used for motion compensation.

Layers of Syntax	Function
Sequence Layer	Random access: context
Group of Pictures	Random access unit: video
Picture Layer	Primary coding unit
Slice Layer	Resynchronization unit
Macroblock Layer	Motion Compensation unit
Block Layer	DCT unit

TABLE 2. Structure of MPEG bit stream

### 2.2.1 Sequence Layer

2.2.2 The Sequence Layer begins with a header followed by one or more Group-of-Pictures (GOP) and ending with an End-of-Sequence code. Each GOP may be preceded by a sequence header. The sequence header contains video information such as the horizontal and vertical picture sizes, pel aspect ratio, picture rate, bit rate, and virtual buffer verifier (VBV) size.

### 2.2.3 Group-of Pictures Layer

A GOP consists of a collection of pictures. A typical format for a GOP is shown in Figure 3. Each GOP contains at least one I frame. B frames within one GOP can reference an I frame in another GOP. The ratio of Inter-coded-to-Intra-coded pictures (N) is equal to the number of B/P frames divided by the number of I frames.

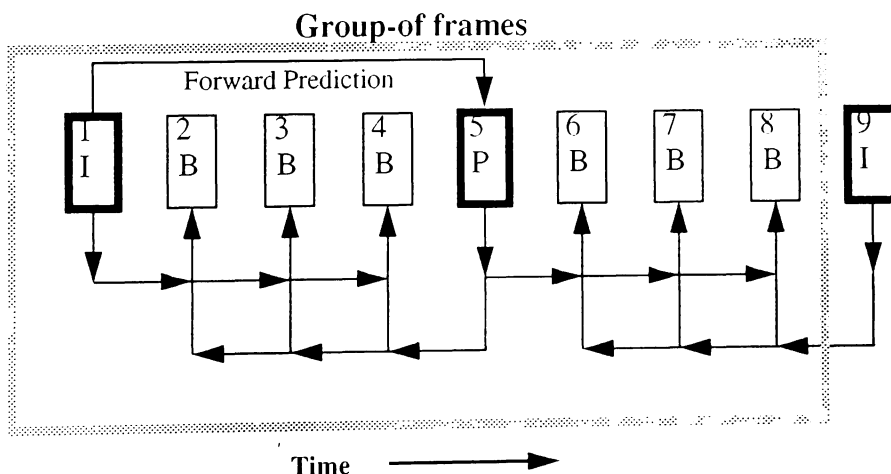


FIGURE 3. MPEG temporal picture structure N=7

## 2.2.4 Picture Layer

There are four type of frames in MPEG: Intracoded (I), Predicted (P), Bidirectional-Predicted (B) and DC frames. I frames are encoded using DCT and IDCT and do not use motion compensation and are referenced by P and B frames. P frames reference a previous I or P frame by using motion compensation. B frames are coded with reference to the previous I or P frame, next I or P frame or both. B frames use motion compensated interpolation. DC frames are encoded using DCT and IDCT, but only use the DC coefficients. This provides a simple, but low quality fast-forward mode. None of the video sequences studied in this paper contained DC pictures.

## 2.2.5 Slice Layer

Each picture is divided into Slices consisting of a Slice header and one or more macroblocks. The Slice header contains the vertical position of the slice within a picture and the quantization scale (q) since Slices can have different quantization scales. Each Slice is encoded without dependence on any other Slice. As a consequence, a Slice is the lowest error-recoverable unit within MPEG. If an error occurs within a Slice, it is possible to recover from the error and not affect the total picture.

The number of Slices per frame is quite flexible and is determined during encode time. A frame can consist of Slices which start at the left side of the picture and end at the right hand side as shown in Figure 4<sup>1</sup>. An alternate format would be to make the Slice start on one horizontal line of the picture and end on another. This is shown in Figure 5. It is possible for a picture to contain only one Slice; however, if an error occurs then the whole picture is affected. The benefit of reducing the number of Slices within the picture is in reducing the header overhead associated with each Slice.

Each Slice consists of a 40 bit header; consequently, the more Slices per picture, the more header bits within a picture. If the video sequence is transported over a very reliable network then this trade-off is acceptable. However, this is not acceptable for VBR video sequences on ATM networks where the likelihood of causing a Slice error due to cell-loss exists. Therefore, a format which divides the picture into multiple Slices is preferable for VBR transmission.

---

1. This is the recommended method of Slice encoding in MPEG-2.

1 Begin	1 End
2 Begin	2 End
3 Begin	3 End
4 Begin	4 End
5 Begin	5 End
6 Begin	6 end
7 Begin	7 End
8 Begin	8 End
9 Begin	9 End
10 Begin	10 End
11 Begin	11 End
12 Begin	12 End
13 Begin	13 End
14 Begin	14 End
15 Begin	15 End

FIGURE 4. Possible Slice arrangement for SIF 352x240 picture.

1 Begin	1 End	2 Begin	
	2 End	3 Begin	
	3 End	4 Begin	
		4 End	
5 Begin		5 End	
6 Begin	6 end	7 Begin	
	7 End	8 Begin	
	8 End	9 Begin	
	9 End	10 Begin	
	10 End	11 Begin	
		11 End	12 Begin
	12 End	13 Begin	
			13 End

FIGURE 5. Alternate Slice arrangement for SIF 352x240 picture.

### 2.2.6 Macroblock Layer

The macroblock is the basic unit of coding for motion compensation. Macroblocks are encoded from the top left-most part of the picture to the lower right-most part scanning from left-to-right and top-to-bottom. Macroblocks consists of a header followed by six component blocks shown in Figure 6. The six component blocks are made from four luminance blocks (Y) and two chrominance blocks Cr and Cb<sup>1</sup>.

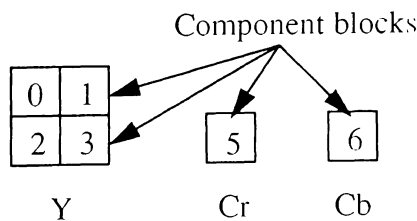


FIGURE 6. Macroblock 4:2:0 structure

The macroblock header contains the macroblock stuffing, address increment, macroblock type, and quantization scale ( $q$ ) fields. Macroblock stuffing is used by the encoder to increase the bit-rate of the data stream in order to avoid a buffer underrun condition. These bits are discarded by the decoder. The macroblock address increment defines the relative position of the macroblock within the current Slice. Macroblocks which are intracoded always have an address increment of 1. Inter-coded macroblocks can have an address increment greater than 1 and are called *skipped* macroblocks. The quantization scale is used to calculate the quantization step for the current macroblock. This is an adaptive quantization technique in that the quantization scale can be different for each macroblock.

The quantization step limits the range of values of the DCT coefficients. For DC coefficients it is fixed at 8, but for AC coefficients it is calculated using the following formula:

$$i[u, v] = 8 \times c[u, v] / q \times m[u, v]$$

In this formula,  $i[u, v]$  is the quantized coefficient matrix,  $c[u, v]$  is the coefficient matrix, and  $m[u, v]$  is the quantization matrix. The quantization matrix could be a default matrix or downloaded in the sequence header. The output bit-rate of the encoder can be varied by changing the quantizer step. This is done by changing  $q$  in either the Slice or macroblock headers.

There are four basic types of macroblocks in MPEG: Intracoded, Forward-Predictive, Backward-Predictive and Bidirectional-Predictive. Intracoded macroblocks (I) use spatial encoding and do not reference any other frame. Forward-Predictive macroblocks (P) use motion compensation and contain a motion vector which points to a macroblock in the previous I or P frame. Backward-Predictive macroblocks (B) contain a motion vector which points to a macroblock in the next I or P frame. Bidirectional-Predictive macroblocks use interpolation and contain two motion vectors which point to macroblocks in the previous and next I or P frames.

The picture type determines the types of macroblocks contained within the frame. For example, I frames only contain I macroblocks while P frames contain both I and P macroblocks. The motion compensation unit must go through a decision process in order to determine which macroblock type to select. The decision as to which macroblock type to

---

1. This is referred to as the 4:2:0 format as opposed to the 4:2:2 format which uses two chrominance blocks or a 4:4:4 format which uses four chrominance blocks. MPEG-1 only uses the 4:2:0 format; whereas, MPEG-2 specifies the 4:2:2 and the 4:4:4 format.

select is roughly based on which one will require the fewest bits to encode. If an appropriate motion vector is found then the macroblock is encoded as a P macroblock; otherwise, it is encoded as an I macroblock. B frames are the most complex and consist of all four macroblock types. They require the most computing power to encode, but offer the highest amount of compression.

### 2.2.7 Block Layer

The Block is the lowest layer in the MPEG architecture. It is the basic coding unit for the DCT/IDCT spatial compression algorithm. Each block consists of 64 pels arranged in an 8x8 structure.

### 2.3 Start Codes

The MPEG bit stream is delimited by the Start Code Prefix and Start Code shown in Figure 3. The Start Code Prefix is a 001 byte pattern which does not occur normally in the bit stream. Once the decoder detects a Start Code Prefix it then decodes the next byte which is the Start Code. Following each Start Code is header information pertaining to that particular layer.

Start Code Name	Hexadecimal Value
Start of Picture	00
Start of Slice (Also slice vertical position)	01 through AF
reserved	B0
reserved	B1
User Data	B2
Sequence Header	B3
Sequence Error	B4
Extension	B5
reserved	B6
Sequence End	B7
Start of Group of Picture	B8
System Start Codes	B9 through FF

TABLE 3. MPEG-I Syntax Start Codes

## 2.4 MPEG Encoder

A simplified diagram of the MPEG encoder is shown in Figure 7. During Intraframe coding, the DCT, Quantizer (Q) and Variable Length Coding (VLC) is used to compress a macroblock. The Inverse Quantizer ( $Q^{-1}$ ) and the Inverse Discrete Cosine Transform (IDCT) are used to develop the frames for reference by motion compensation. The bit-rate is assumed to be constant and is specified in the sequence header.

The Virtual Buffer Verifier (VBV), shown at the output of the encoder, is a buffer monitored by the Regulator to insure that an overflow or underflow condition does not occurs. If the VBV is approaching an underflow condition, stuffing bits are added by specifying a macroblock stuffing code in the macroblock header. These stuffing bits are removed at the decoder. The stuffing bits effectively increase the bit-rate of the encoded output stream. If the Regulator senses an overflow condition, the quantizer will increase the quantization scale. This will effectively decrease the bit-rate of the output stream.

The size of the buffer is specified in the sequence header and is sent to the decoder. The basic idea is that if a CBR channel is allocated using the bit-rate and the buffer size, which is specified in the sequence header, then there is an implicit guarantee that the buffer will not overflow or underflow.

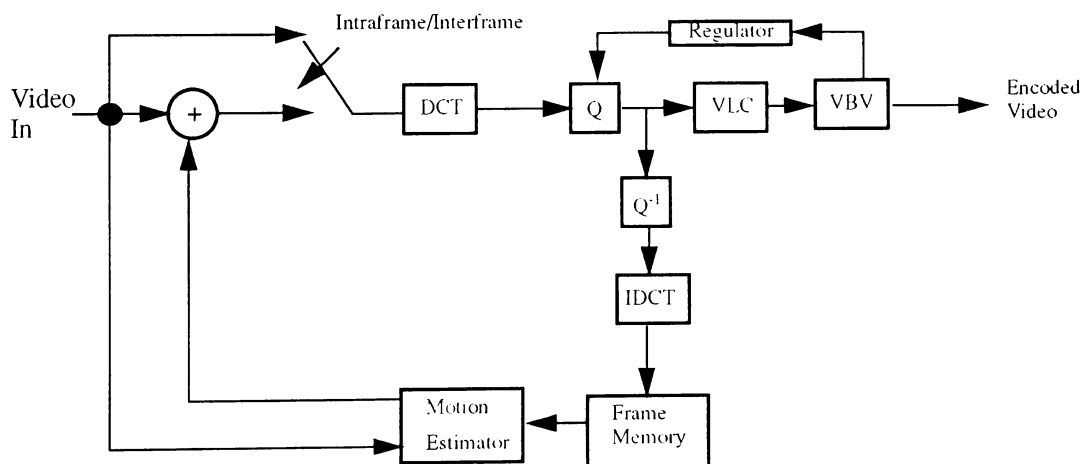


FIGURE 7. Simplified block diagram of MPEG encoder

## 3.0 Previous Work in Video Modeling

Proposed models have fallen into three categories: Auto Regressive (AR), Markov, and mixed AR and Markov. Most researchers have developed models at the Picture Layer

using AR(1) and AR(2) models. The Markov Chain has also been used, in particular the Markov Modulated process with batch arrivals. Recently, ARMA models has been used to model video. A block level model was recently developed using multiple AR(1) processes with time-varying parameters controlled by a Markov Chain.

The AR(2) model has been shown to produce good results in capturing the bit and cell rate statistics at the Picture Layer for video conference type video with little motion. The coefficients for this model are simple to estimate from the empirical data using the autocorrelation coefficient at lag 1. AR models, in general, appear to capture the autocorrelation behavior of compressed video sources which is an important prerequisite for any model of compressed video sources.

ARMA models have recently been used to model video sources. The difficulty with this model: however, is in calculating the MA coefficients. Also, to model video at the Slice layer would require MA coefficients about equal to the number of slices per picture. This means that for the video sequences studied in this paper an ARMA(2,15) would be required which involves the calculation of 17 coefficients.

Markov Chains provide a compact way of generating the probability distribution function which fits the video data well. The process of calculating the state transition probabilities is straight-forward. We will see later in this paper than an 8-state Markov Chain fits the video data well. It does appear that one can model video at lower layers than the Picture layer using a Markov Chain. Markov Chains also tend to capture the correlated behavior of the data well.

While it seems that the AR(2) process is a good model at the Picture Layer, it does not appear that this model is sufficient for video sequences containing sudden scene changes. It also appears that pure AR video models are not sufficient to capture the behavior of video data containing I/B/P frames. As a consequence, recent work proposes models which use a mix of AR processes controlled by a Markov Chain. Here, AR coefficients vary in time according to a Markov Chain. It appears that this type of model would involve the fewest coefficients. This type of model was used to model video at the Macroblock layer and seems very appropriate to model video lower than the Picture layer.

### 3.1 AR Process Overview

Many authors have modeled the bit-rate behavior of compressed video using the AR process. In general, the form of the AR(p) process of order p is,

$$X(n) = \sum_{i=1}^p \phi_{p,i} X(n-i) + e(n)$$

where  $X(n)$  is a random variable and  $\phi_{p,i}$  are the coefficients of the AR processes and are not equal to zero. The variable  $e(n)$  is a sequence of independent and identically distributed Gaussian random variables with zero mean<sup>1</sup>.

The coefficients for the AR(p) process are calculated using the Yule-Walker equations shown below.

$$\begin{bmatrix} r_{XX}(1) \\ r_{XX}(2) \\ * \\ r_{XX}(p) \end{bmatrix} = \begin{bmatrix} r_{XX}(0) & r_{XX}(1) & r_{XX}(2) & r_{XX}(p-1) \\ r_{XX}(1) & r_{XX}(0) & r_{XX}(1) & r_{XX}(p-2) \\ * & * & * & * \\ r_{XX}(p-1) & r_{XX}(p-2) & * & r_{XX}(0) \end{bmatrix} \begin{bmatrix} \phi_{p,1} \\ \phi_{p,2} \\ * \\ \phi_{p,p} \end{bmatrix}$$

Using matrix notation, we let  $R$  equal the autocorrelation coefficient matrix and  $r_{XX}$  be the correlation vector then,

$$r_{XX} = R\Phi$$

where  $\Phi$  is the AR coefficients vector. This is called the Yule-Walker equation. We can calculate the AR coefficients by using the following equation since the matrix  $R$  is invertible.

$$\Phi = R^{-1}r_{XX}$$

---

1.  $e(n)$  is often called white noise or white Gaussian noise.

An extension of the AR process is the Autoregressive Moving Average (ARMA) process. The ARMA process differs from the AR process in that an extra term called the Moving Average (MA) is added. The ARMA process equation is as follows,

$$X(n) = \sum_{i=1}^p \phi_{p,i} X(n-i) + \sum_{k=1}^q \theta_{q,k} e(n-k) + e(n)$$

The second part of the ARMA equation represents the Moving Average. It consists of weighted samples of previous values of the white gaussian function,  $e(n)$ . The weighting values are the coefficients  $\theta_{q,k}$ . ARMA models are identified by two parameters  $p$  and  $q$ , where  $p$  is the order of the AR process and  $q$  is the order of the MA process. The coefficients  $\phi$  and  $\theta$  are derived empirically.

### 3.1.1 Previous work using AR models

Nomura, et al. [13] video was modeled as a first order AR process. Two, 20 second video sequences were analyzed. One sequence was an active scene and the other an inactive scene. They suggested modeling video using multiple AR processes where a Markov-Chain was used to determine which AR process was active. Zdepski, et al [14] modeled several video sources using a first order synthesis lattice filter driven by white gaussian noise. The video sources were encoded according to the H.261 standard. The process parameters were extracted from the video data. The model was constructed to analyze the bit-rate behavior of the video source at the frame level. The bits per Group-of-Block (GOB)<sup>1</sup> was determined by dividing the bits per frame value, gotten from the model, by 12. This assumed that each GOB were the same size. They stated that a 12-th order model was required to accurately capture the autocorrelation of the data since there are 12 GOB per frame.

In Grunenfelder [15], video was modeled as an ARMA process. He presented a mathematical model consisting of a transverse filter of finite order, a recursive filter, and a memory-less nonlinear cell interarrival sequence which is assumed to be Wide-Sense Stationary (WSS). The transfer function is calculated such that when white noise is applied to the input of the filter, the output is the cell interarrival sequence exhibiting the same mean, variance and autocorrelation of the empirical sequence. Bragg and Chou [16] examined the implications of modeling video using ARMA models. They stated that sampling an

---

1. The GOB in H.261 is similar to the slice in MPEG.

ARMA model using longer time intervals was still an ARMA model. Specifically, it appears that as the sampling interval increased the order of the AR component of the ARMA process increased while the MA order decreased. They also pointed out that video stream monitors do not have to sample every picture time (1/30 sec) in order to observe the general ARMA characteristics of the stream. They also stated that ARMA(p,q) streams sampled every k time units will tend towards ARMA(p,p) or ARMA(p,p-1) for large k.

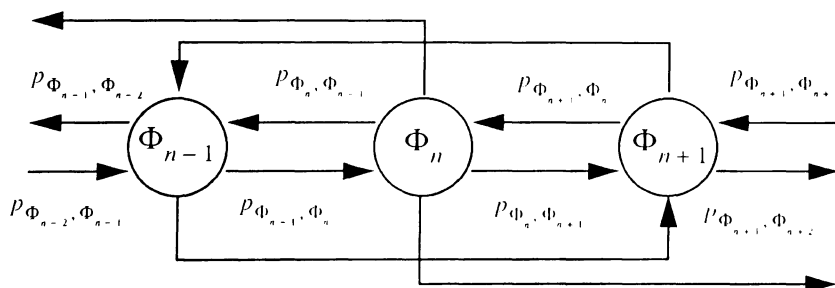
Jabbari, et al. [17] developed a composite of first-order statistically dependent AR processes to represent the number of bits per frame for encoded full-motion video. They used a video sequence consisting of 350 frames to develop their model. The video sequence conformed to the general MPEG syntax and not contain B frames. They used two AR processes for each block type, the first for the number of blocks per field and the second for the number of bits per block. The AR models were derived using only first and second order statistics and correlation coefficients of one field lag. A Markov Chain was used to vary the coefficients of the AR process over time. They found that statistics matched the empirical data well and that the number of bits per block for each block encoding scheme was a Gaussian distribution.

### 3.2 Markov Chain Overview

A Markov chain can be used to capture the bit-rate behavior of a encoded video sequence. Each state would represent the amount of data per frame or slice. Data could be in bits, bytes or cells. This method requires empirical data in order to derive the state transition probability matrix. The transition probability in general is calculated by the following relation.,

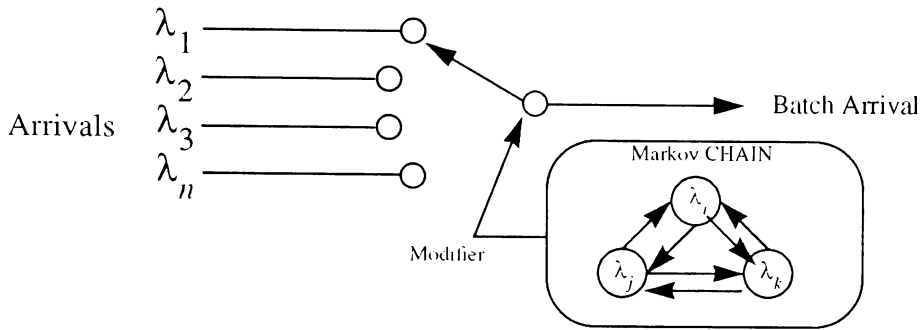
$$P_{ij} = \frac{\text{Number of transitions from } i \text{ to } j}{\text{Number of transitions out of } i}$$

In general the Markov chain takes the following form,



In order to reduce the number of states within the Markov chain some researchers have divided the amount of data within a picture by a constant. This essentially makes the state of the Markov chain equal to a range of data values instead of a single data value.

Another form of the Markov chain is the Markov Modulated process with batch arrivals. The state of the Markov chain determines which arrival process is selected. This model is useful when the bit-rate varies according to specific classes of picture content such as scenes with no, medium or fast motion. A diagram of this process is shown below.



### 3.2.1 Previous work using Markov Chains

Maglaris, et al [18] used an AR(1) and a Markov chain to model compressed video. The AR(1) process was used for simulation and the Markov chain was used for queueing analysis. The Markov chain was discrete-state and continuous-time. Huang [19] proposed a discrete-time, discrete-space Markov Chain to model the aggregate packet-rate process. Thirty different video sequences were analyzed using interframe and intraframe coding. The interframe coding consisted of taking the difference between adjacent frames and encoding it. Motion compensation was not used. Yasuda, et al. [20] analyzed three video sequences each 15 minutes long. He pointed out that it is difficult to estimate traffic characteristics by combining an AR model with an analytic technique. As a result, he proposed a Markov Modified Poisson Process (MMPP) which included batch arrivals as a model for network analysis. Sen et al. [21] used a correlated Markov model to analyze video sources encoded using conditional replenishment interframe coding. They studied video data with multiple activity levels leading to sudden changes in output bit rate. They also pointed out that there was a smoothing effect when multiplexing several VBR sources.

Heyman, et al. [22] analyzed a long video sequence of 48,500 pictures at the cells per picture level. They proposed that the Gamma distribution fit the Cells/Frame distribution well. They suggested that possibly a mixture of Gamma and Exponential distributions might result in a more accurate distribution. They also showed that an AR(2) process pro-

duced too few cell losses in simulation and that a Markov chain model was a good source model for congestion studies. Skelly, et al [23] developed a model based on the arrival-rate histogram of the video source. They calculated the histogram of the aggregate arrival-rate by taking the convolution of the individual arrival-rate histograms. They used a Markov Modulated Poisson Process to accurately model the queueing behavior of the video multiplexer. Their results indicate that the form of the autocorrelation function is not important.

In Yegenoglu, et al. [24] the bit rate per picture of the VBR video source was modeled as the superposition of two independent AR processes to capture the autocorrelation. A third process was added to account for the extra bits generated during scene changes. They used a discrete Markov chain to capture the long-term bit-rate behavior of full motion video and showed that the bit-rate histogram for the aggregate bit rate tends toward a Gaussian distribution. They studied a single video sequence of 500 pictures in CCIR 601 format with 720 x 480 pixels per picture and a picture rate of 30 pictures per second.

### 3.3 Empirical Models

The Time Event Sample (TES) method is well suited for modeling general autocorrelated time series. It can model marginal distributions exactly and approximate the autocorrelation behavior. This technique is computational intensive; thereby, requiring software tools. This technique is heuristic and requires a sample of the data to model. In Melamed, et. al. [25] a TES model was used to characterize the video data; however, this model relies on empirical data. TES models do appear to capture the autocorrelation characteristics of the data and match the distribution exactly.

Rodriguez, et. al. [26] used a method where key parameters were extracted from the video source which were independent of the encoder. These parameters captured the basic characteristics of the video sequence and allowed for the characterization of video independent of the encoding scheme. A linear function used these parameters to model the video source.

## 4.0 Experimental Investigation of MPEG Slice Statistics

Three high-quality MPEG encoded VBR video sequences were studied. They are called *Bike*, *Flowg* and *Tennis*. The video sequences were obtained from the Stanford FTP (File Transfer Protocol) site repository. One can gain access to the Stanford repository by using anonymous FTP to the Internet address *havefun.stanford.edu*. Once logged in, you can

change directories to */pub/mpeg* to obtain the video files. Each video sequence was encoded using both predictive and interpolative motion compensation (contain I/B/P frames).

The MPEG software decoder, called *mpeg\_play*, was used to view the video sequences. The decoder was obtained from the University of California at Berkeley using the Internet. The FTP site address is *toe.cs.berkeley.edu*. The files are located in the directory */pub/multimedia/mpeg*. The video sequences were displayed on an IBM RS/6000 workstation configured as an AIX Client running AIX version 3.2 under AFS (Andrew File System). The average picture display rate was between 2 and 5 pictures per second. Stanford University also provides an MPEG codec which was used to decode the video sequences and output YUV files. The size of these files was used to calculate the compression ratio.

A program called *MPEGAnalyzer* was written to parse an MPEG-1 video sequence according to the MPEG syntax. The program scans the file for the Start-Code Prefix consisting of a three byte *001* hex value followed by a one byte Start-Code. Once the Start-Code is found, the Start-Code header is decoded and pertinent information within the header is written to an output file. Information is extracted from the Sequence header such as the picture size, pel aspect ratio, picture rate and bit rate<sup>1</sup>. A record is printed for each slice specifying the vertical position of the slice within a frame, the number of bytes in the slice, the number of ATM cells within the slice and the quantization level of the slice. Each slice was segmented into 48 bytes of an ATM cell payload. The picture type, GOP number, slice and frame statistics were printed for each frame. At the end of the video sequence, *MPEGAnalyzer* prints the aggregate slice and frame statistics and the probability mass function is plotted for the number of cells/slice and the number of cells/picture.

#### 4.1 Description of the Video Sequences

Each sequence contains a total of 150 pictures and had a picture rate of 30 pps (pictures per second). All video sequences were high quality encoded with the quantization scale,  $q=4$  for I and P frames and 8 for B frames. The Inter-coded-to-Intra-coded picture ratio,  $N$ , is equal to 5. There are six pictures per GOP consisting of an I frame, followed by two B frames, a P frame and finally two more B frames (.IBBPBBI.). Each picture consists of 15 slices where the format is similar to that shown in Figure 5 only. The only difference is

---

1. The bit-rate is an 18 bit integer measured in units of 400 bits/second. A bit-rate value of "3FFFF" hex specifies a variable bit-rate.

that there are an extra two slices per picture. All sequences consists of 26 I frames, 25 P frames and 99 B frames.

The first video, called *Bike*, is a 5 second sequence from the movie *Terminator II*. This sequence shows a rider on a motorcycle jumping from a ramp onto a cement canal bed. The sequence begins with the motorcycle located in the upper right-hand corner of the picture. The motorcycle starts out as a small object which grows when the camera zooms-in from the front. The motorcycle covers most of the picture when it hits the floor of the canal. The final pictures in the sequence shows an abrupt scene change to a close-up of the rider's head. The main attributes of this sequence are the zoom-in, abrupt scene change and the close-up.

The second video is a 5 second sequence called *Flowg* (Flower Garden). This sequence showed a flower garden covering the lower half of the picture and a row of houses in the background covering the upper half of the picture. The garden consists of small red, yellow, purple and white flowers. The garden is on a mound which slopes up and away from the camera. The camera is panning the scenery from left-to-right. The main features of this sequence are the multitude of small objects (flowers), coloring and camera panning.

The last video is a 5 second sequence called *Tennis* which shows two men playing table-tennis. The opening scene shows a close-up of a ping-pong ball bounced by one of the players. As he begins to play, the camera zooms-out and shows half of the ping-pong table; the other player is not yet visible. Midway through the sequence there is a sudden scene change to show the other player. The other player returns a few shots and then the sequence ends. The main characteristics of this video sequence is the close-up of the bouncing ping-pong ball, the zoom-out and the scene change.

*Tennis* and *Flowg* were extracted from CCIR-601 originals and decimated using the MPEG SM-3 decimation filter. The CCIR recommendation 601 defines standards for the digital coding of color television signals in YUV<sup>1</sup> component form used for studio quality TV. The size of the picture is 720x480 pixel per field at a field rate of 60 fields per second interlaced scanning. To convert to SIF the odd fields of the CCIR-601 original are decimated horizontally for luminance and both horizontally and vertically for chrominance. Decimation involves the subsampling of the CCIR-601 original of 720x480 pixels @ 30 fps to obtain the SIF picture size of 352x240 pixels. MPEG requires that the input to the encoder be SIF. *Bike* was extracted from laserdisc and digitized by an Abekas A-20. It was

---

1. Y represents luminance samples and U, V chrominance samples.

then converted from CCIR-601 to SIF in the same manner as *Flowg* and *Tennis*. All of the video sequences were coded using the standard MPEG quantization tables with variable length codes. The motion estimation is full-search on an integer pel grid, which is approximately a +/- 7 pel displacement, and then a half-pel local search was done.

#### 4.2 Picture Density and Compression Ratio

To compare the video sequences quantitatively two metrics are used: picture density and video compression ratio. The picture density is calculated using the following formula,

$$D = \frac{F_c}{N} \quad (1)$$

where,

- D = Picture Density (bytes/picture)
- $F_c$  = Compressed file size (bytes)
- N = Number of pictures in the video sequence

Given video sequences encoded with the same values of N and q, picture density gives an indication of the effectiveness of the compression technique.

The compression ratio is a ratio of the size of the uncompressed video sequence to the compressed video sequence. The formula for the compression ratio is,

$$C = \frac{F_u}{F_c} \quad (2)$$

where  $F_u$  is the size of the uncompressed file and  $F_c$  is the size of the compressed file. The following formula is used to calculate  $F_u$ ,

$$F_u = N \left( R + 2 \left( \frac{R}{4} \right) \right)$$

$$F_u = \frac{3(N \times R)}{2} \quad (3)$$

where,

R = Size of the picture in pixels (where 1 pixel = 1 byte)

This formula assumes that each pixel consists of a one byte sample for each component. We have one luminance sample per pixel and two chrominance sample for every four luminance samples. Using this formula, we calculated the size of the uncompressed video sequence for all three videos. The results were verified using the output of the Stanford

software decoder. Since the picture size and the number of pictures is the same for all three videos, we can calculate  $F_u$  once and use it to calculate the compression ratio for all three video sequences.

$$F_u = 150 \text{ pictures} \times \frac{3 \times 352 \times 240}{2} \text{ bytes/picture}$$

$$F_u = 150 \times (126,720) = 19,008 \times 10^6 \text{ bytes}$$

Using  $F_u$  we can now calculate the compression ratios for each of the video sequences.  $F_c$  was obtained from Table 4.

$$C_{Bike} = \frac{19,008 \times 10^6}{642,583} = 29.581$$

$$C_{Flowg} = \frac{19,008 \times 10^6}{2,819,836} = 6.741$$

$$C_{Tennis} = \frac{19,008 \times 10^6}{1,246,001} = 15.255$$

Note that the picture density and compression ratio are related by the following formula,

$$D = \frac{F_u}{N \times C} \quad (4)$$

The picture density and compression ratios of the three video sequences was calculated and tabulated in Table 4. *Bike* had the highest compression ratio of the three video sequences. It would appear that the motion compensation compression technique used by MPEG was most effective for the type of scene content within *Bike*. *Flowg* had the lowest compression ratio of the three video sequences. Obviously, the motion compensation technique did not work as well as it did with *Bike*. We tried to get a better understanding of the differences in compression ratio by looking at the macroblock type distribution within each picture type

Video Name	File Size (Bytes)	Total Pictures	Mean Picture Density	Compression Ratio
<i>Bike</i>	642,583	150	4,284	29.581

TABLE 4. MPEG video file quantitative information

Video Name	File Size (Bytes)	Total Pictures	Mean Picture Density	Compression Ratio
<i>Flowg</i>	2,819,836	150	18,797	6.741
<i>Tennis</i>	1,246,001	150	8,306	15.255

TABLE 4. MPEG video file quantitative information

### 4.3 Macroblock Type Distribution

The distribution of the macroblock type within P and B frames gives an indication of the effectiveness of motion compensation. The more I macroblocks within P and B frames the less effective motion compensation was in finding appropriate motion vectors. I frames will always have the same number of I macroblocks per picture. P frames will have a mix of I and P macroblocks while B frames will have a mix of I, P, B and Bi macroblocks. The number of bits per picture depends on the macroblock type selected and the number of bits per macroblock. Macroblock type selection is based on the motion content of the video sequence. For example, when encoding B frames, the encoder attempts to encode the current macroblock as a Bi macroblock. If a Bi macroblock is not appropriate, then the encoder will try to encode it as a P or B macroblock. As a last resort, the encoder will encode the macroblock as an I macroblock. The same strategy is used to encode P frames except the encoder chooses between P and I macroblocks. The more I macroblocks contained within P and B frames the more bits contained in the picture.

Table 5 shows the mean number of macroblock types per picture type. These *Bike* had P frames with the lowest mean number of I macroblocks and B frames with the second lowest. One possible reason for this is that for most of the video sequence a small moving object was in the foreground and the background consisted of large surface areas where predictive encoding and interpolation should do well. *Flowg* had B frames with the highest mean number of I macroblocks. *Flowg* consisted of scenery which was panned and contained a multitude of small objects possibly causing mismatches when using predictive or interpolative encoding. *Tennis* had B frames with the lowest mean number of I macroblocks and P frames with the highest mean number of I macroblocks. This would indicate that Backward-Prediction worked well, but Forward-Prediction did not when compared to the other video sequences. It is interesting to note that *Flowg* had the lowest compression ratio and *Bike* had the highest. One can infer that the distribution of I macroblocks in P and B frames has an affect on compression ratio.

Picture =>	I	P		B			
Macroblock =>	I	I	P	I	P	B	Bi
<i>Bike</i>	330	5.76	324.12	1.42	47.22	57.52	216.60
<i>Flowg</i>	330	15.8	304.24	79.02	52.34	58.17	213.14
<i>Tennis</i>	330	22.96	302.72	0.85	29.43	66.03	218.12

TABLE 5. Mean number of macroblock types per picture type

#### 4.4 Video Sequence Statistics and Autocorrelation Function

Table 6 shows the cells/slice statistics for the three video sequences. *Bike* had the highest peak-to-mean ratio which would indicate a proportional relationship between the compression ratio and the peak-to-mean ratio. *Flowg* had the lowest peak-to-mean ratio and the lowest compression ratio. Note that for *Bike*, *Flowg* and *Tennis* sequences the minimum cells/slice is one standard deviation away from the mean while the peak multiple standard deviations away. We shall see in the next section that this fact might present a problem for symmetric dynamic bandwidth allocation schemes. AllMux is a time-shifted multiplex of the three video sequences and will be discussed later.

Video Name	Peak	Mean	Std. Dev.	Variance	Coeff. of Variation	Peak/ Mean
<i>Bike</i>	40	6.4351	7.0445	49.6243	1.0947	6.2159
<i>Flowg</i>	105	26.6080	25.7041	660.6982	.9660	3.9462
<i>Tennis</i>	53	12.0204	13.1238	172.2344	1.0918	4.4092
<i>AllMux</i>	115	44.1887	21.5027	462.3659	.4866	2.6025

TABLE 6. MPEG ATM Cells/slice statistics

The peak number of cells/slice is determined by the maximum number of cells/slice contained within I frames. Referring to Figure 15, we can see that the shapes of the peaks for each of the video sequences is a result of the affect of picture content on the spatial encoding of the I frames. Pictures which contain many objects will generate I frames whose macroblocks generate many non-zero AC coefficients. This reduces the effectiveness of the run-length encoding and increases the number of bits per macroblock. For example, the *Bike* sequence begins with the motorcycle located in the top-half of the picture. The result is an I picture where the largest slices occur at the top of the picture (slices at the top of the picture are located at the left-hand side of the peak). *Flowg* has flowers covering the bottom half of the picture resulting in the larger slices occurring on the right-hand portion of the peak. We can also see that for this portion of the sequence approximately 90 cells/

slice were required to encode the bottom portion of the picture. Clearly, this is a result of the increased number of non-zero AC coefficients. *Tennis* has a relatively flat peak. This is due to the fact that the opening scene of this video sequence is a close-up of a bouncing ping-pong ball. Since the ball covers most of the picture, the number of non-zero AC coefficients is fairly constant for each slice within the picture.

The bit-rates can be calculated from the cells/slice data by using the following formula.

$$B = (30 \frac{\text{pictures}}{\text{second}}) \times (53 \frac{\text{bytes}}{\text{cell}}) \times (15 \frac{\text{slices}}{\text{picture}}) \times (S \frac{\text{cells}}{\text{slice}}) \times (8 \times 10^{-6} \frac{\text{Mb}}{\text{byte}})$$

This formula simplifies to the following.

$$B = 0.1908 \times S \quad \text{mbps} \quad (5)$$

Using this formula we can calculate the peak and mean bit-rates for the video sequences which are shown Table 7. We can see that the bit-rates can vary from 1.228 mbps to 20.034 mbps for these video sequences.

Videos	Peak Rate	Mean Rate
<i>Bike</i>	7.632	1.228
<i>Flowg</i>	20.034	5.077
<i>Tennis</i>	10.112	2.293

TABLE 7. Bit-rate in megabits per second

The autocorrelation function for the three video sequences is shown in Figure 16. It is strongly correlated and periodic, decaying with a negative slope with increasing lag. Peaks in the autocorrelation function occur every 45 slices which is due to the occurrence of I and P frames. The peak period is due to the number of B frames there are between I and P frames. This is illustrated more closely in Figure 17. It does appear that the frame sequence dominates the correlation function rather than the picture content. Livny, et. al. [27] points out that correlated sources can significantly degrade queuing performance. One would have to conclude that these video sequences are highly correlated and would present problems for queueing systems. This raises the question as to whether statistically multiplexing such sources makes sense. We address this issue later on when we discuss time shifted multiplexing.

## 4.5 Statistical Distribution

Early research work indicated that the video picture bit rate had a Normal Gaussian type distribution [13], [17]. While this was true for video conference type sequences containing little motion, recent work shows that the distribution of the number of ATM cells/picture had a Gamma distribution [22], [28] for video sequences with motion and scene changes. Pancha et. al. [9], pointed out that the Gamma distribution fits the cells/slice distribution well for low quality sources ( $q=16$ ), but did not fit well for higher quality sources ( $q=4,8$ ). Kishimoto et al. [29] and Heyman et al. [22] pointed out that a more accurate distribution might be a combination of distributions. The former proposed a mix of three Gaussian distributions while the latter proposed a mix of Gamma and Exponential distributions. Both did not characterize video at the Slice layer. These studies did not include video sequences with B frames and only contained I and P frames.

We attempted to determine if a video sequence, containing B frames, cells/slice distribution would fit the Gamma distribution. The continuous version of the Gamma probability density function (pdf) is given by the following equation:

$$f(x) = \frac{\lambda (\lambda x)^{\alpha-1}}{\Gamma(\alpha)} e^{-\lambda x} \quad (x \geq 0) \quad (6)$$

where  $\Gamma(\alpha)$  is the Gamma function defined by the following integral

$$\Gamma(\alpha) = \int_0^{\infty} x^{\alpha-1} e^{-x} dx \quad (7)$$

The Gamma density function parameters,  $\alpha$  and  $\lambda$ , are estimated by using the Method-of-Moments [30]. This method estimates the parameters a pdf by taking the  $n$  moments of the data where  $n$  is the number of parameters to estimate. In the case of the Gamma Function, there are two parameters to estimate; therefore, two moments are required. The first and second moments of the Gamma function are,

$$\mu_1 = \frac{\alpha}{\lambda} \quad \mu_2 = \frac{\alpha}{\lambda^2} + \frac{\alpha^2}{\lambda^2}$$

Solving for  $\alpha$  and  $\lambda$  we get the following equations:

$$\alpha = \frac{\mu^2}{v} \quad \lambda = \frac{\mu}{v}$$

where  $\nu$  is the variance  $\mu$  is the mean. The Gamma pdf for each of the video sequences was generated using the estimated values for  $\alpha$  and  $\lambda$  shown in Table 8. Note that as  $\alpha$  approaches 1, the Gamma pdf simplifies to an Exponential distribution shown in (8).

$$f(x) = \lambda e^{-\lambda x} \quad (x \geq 0) \quad (8)$$

Figure 18 shows the histograms for the cells/slice distribution for *Bike*, *Flowg* and *Tennis*. The x and y axis are normalized for comparative purposes. Note that all of the video sequences have a distinctive exponential shape. The estimated Gamma pdf is overlaid onto the histogram plot. There are significant gaps which exist where the Gamma pdf overestimates the number of cells/slice between the x-axis values 0.2 to 0.4. This would indicate that these video sequences will not fit the Gamma distribution. We confirm this by using the QQ plot technique.

Video Sequence	$\alpha$	$\lambda$
<i>Bike</i>	0.8345	0.1297
<i>Flowg</i>	1.0716	0.0403
<i>Tennis</i>	0.8389	0.0698
<i>AllMix</i>	4.0988	0.0910

TABLE 8. Gamma pdf parameters.

The QQ plot [31] is used to determine if two sets of data have the same distribution. This method involves taking the cumulative distribution function (cdf) of both sets of data and comparing their x-axis values for a given y-axis value. This is illustrated in Figure 8. The  $x_1$  and  $x_2$  values are plotted with  $x_1$  values on the x-axis and  $x_2$  values on the y-axis. The values  $x_1$  and  $x_2$  are referred to as the quantiles. If the two sets of data have the same distribution, then the QQ plot will show the  $(x_1, x_2)$  points forming a straight line.

We can see from the QQ plots in Figure 20 that while *Bike* fit the Gamma distribution well both *Flowg* and *Tennis* did not. It is interesting that *Bike* had the highest compression ratio, but cannot claim there is a correlation between compression ratio and the Gamma distribution without study further video samples. It does appear; however, that a single distribution will not fit VBR video containing I/B/P frames.

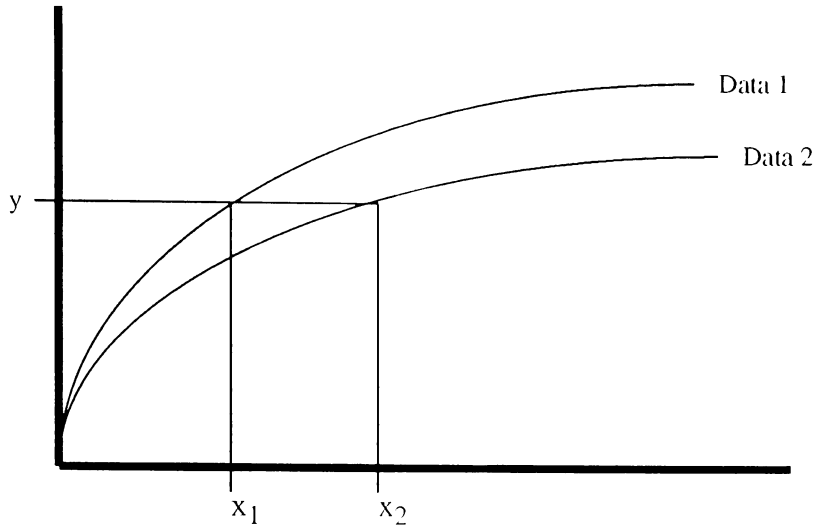


FIGURE 8. Illustration of generating QQ plot coordinates

## 5.0 Impact on Dynamic Bandwidth Allocation Schemes

Referring to Figure 15, we can see that sequences which include B frames produce distinctive peaks-and-valleys in the cells/slice plot. The peaks are caused by I and P frames and the valleys by B frames. The peaks are 15 slices wide and the valleys are 30 slices. There is an abrupt increase in the number of cells/slice when the sequence goes from B frames to I or P frames. This behavior makes it difficult for a traffic predictor to determine when to request additional bandwidth if only the raw video bit stream is monitored. If the traffic predictor monitors the number of cells per frame of all I/B/P frames, it could falsely predict that more bandwidth is required.

In Pancha, et al [9] a simple method, shown in (9), was used to predict whether extra bandwidth was required.

$$\bar{c}_n = \max(\mu, c_{n-1} + \Delta) \quad (9)$$

The estimator  $\bar{c}_n$  represents the number of cells for frame n given  $c_{n-1}$  cells occurred in frame n-1. The value  $\Delta$  is the threshold and was set to one standard deviation. The assumption was that the probability that the number of cells per frame exceeded one standard video between frames was very small. While this is true for video conference type sequences containing only I/P frames, Figure 15 clearly shows this is not the case with I/

B/P frame sequences. As a consequence, the traffic predictor must be selective in the frames it chooses to monitor. We propose that monitoring I frames or slices within I frames would be sufficient for traffic prediction since I frames contain the largest number of cells and provide a strong indication of significant spatial content changes. We can see from Figure 14 that if the three video sequences were concatenated, there would be distinct changes in the I frame peak cells/slices between *Bike*, *Flowg* and *Tennis*. An allocation of 6.678 mbps would be sufficient for *Bike*, 19.08 mbps for *Flowg* and 9.540 mbps for *Tennis*.

## 6.0 Time-Shifted Multiplexing of the Video Sequences

When looking at the cells/slice data shown in Figure 15 one cannot help but notice the distinct peaks and valleys generated by an I/B/P stream. This causes the autocorrelation function to not only be strongly correlated, but periodic as well. This characteristic appears to be consistent amongst the three video sequences. This characteristic would appear to cause problems when multiplexing multiple VBR streams with I/B/P frames. Since the streams are periodic and not statistical in terms of arrivals, if the streams are multiplexed improperly significant inefficiencies in bandwidth utilization might occur. An example would be if we multiplexed the three video streams where I frames overlapped. Since each sequence has the same I/B/P frame pattern, I frames will always overlap for the duration of playback. For this reason, we look at a way to multiplex VBR I/B/P video streams which attempts to take advantage of this periodic behavior. We called this method *Time Shifted Multiplex* or TSM.

We looked at what the effect of multiplexing the three video sequences would have on the resultant cells/slice statistics. We generated the sequence called *AllMux* which is a TSM of the three video sequences. This sequence is generated by shifting the cells/slice data so that I or P frames from one sequence would overlap B frames from another sequence. Each of the sequences were contained in a vector consisting of the number of cells/slices. *Bike* was not shifted. *Flowg* was shifted forward in time by 15 slices and *Tennis* by 30 slices. The resultant vectors were added together and the first 30 slices were truncated to form the new *AllMux* vector. The first two pictures were discarded since they were adjacent I and P frames which occur only during the beginning of playback.

The results in Table 6 shows that the coefficient-of-variation and peak-to-mean ratio are 0.4866 and 2.6025 respectively, which is lower than any of the video sequences. We see from Figure 21, that the plot of the number of cells/slice does not have the distinctive

peaks and valleys shown for the non-multiplexed sequences. Also, the distribution tends to be more Gamma-like than Exponential. The QQ plot confirms this by showing quantile points which tend to fall form a straight line.

The drawback to this approach is that video streams would need to be delayed by the video server in order to insure proper overlap of frames. This can cause problems where frames are not delivered to the client in time for playback, thereby causing frame slips. It might be possible; however, to delay frames given certain delay constraints which will avoid this problem. Also, if a video server has might have some control as to when to start playback of multiple video streams and offset them in order to overlap properly. These issues require further investigation and study. In essence, it does appear that statistically multiplexing VBR video with I/B/P frames does not make sense.

## 7.0 Video Model Using Markov Chain

We used an 8-state discrete-time, discrete-state Markov Chain as a model for the three video sequences and the multiplexed sequence. We attempt to see if the pdf generated by the Markov Chain produces a better fit for the cells/slice distribution. The number of states was selected based on the ratio of the peak cells/slice and the standard deviation. For example, *Bike* had a peak of 40 cells/slice and a standard deviation of 7.0445 cells/slice. This gives a ratio of 5.68:1 which we approximated to 6:1 which would mean using a 6 state Markov Chain; however, we chose 8 states for more accuracy.

Each state represents a range of the number of cells/slice. The range was calculated by taking the peak number of cells/slice and dividing it by 8. So for *Bike* the range of cells/slice is 40/8 or 5 cells/slice. The ranges shown in Table 9 define the discrete-state of the Markov Chain. For example, if the number of cells/slice in the *Flowg* video is 60, the Markov Chain would be in state 4. We used the same number of states for all of the video sequences so that we could compare their steady-state distributions.

Given the states of the Markov Chain defined in Table 9, we calculated the transition probabilities which is shown for *Bike*, *Flowg* and *Tennis* in Figure 9, Figure 10 and Figure 11. The transition probability,  $p_{ij}$  specifies the probability to go from state  $i$  to  $j$ . We can see by looking at the diagonal of the matrices that there is a high probability of the sequence staying in the same state. Also, there is a high probability of being in state 0. This is caused by the B frames. Figure 12 shows the steady-state probabilities for the three video sequences. This represents the pdf of the Markov Chain. Steady-state occurred after 46, 56

and 80 transitions for *Bike*, *Flowg* and *Tennis* respectively. We calculated the steady-state probabilities by multiplying the matrix  $n$  times until all the column transition probabilities were the same. In Figure 22, we compared the steady-state probabilities to the histogram data. We can see that the pdf produced by the Markov Chain is a better fit than the Gamma pdf. Specifically, the gap which existed between x-axis values 0.2 and 0.4 is much less pronounced.

<i>Markov Chain State</i>	<i>Bike</i>	<i>Flowg</i>	<i>Tennis</i>	<i>AllMux</i>
0	0-5	0-14	0-7	0-15
1	6-10	15-28	8-15	16-30
2	11-15	29-42	16-22	31-45
3	16-20	43-56	23-29	46-60
4	21-25	57-70	30-36	61-75
5	26-30	71-84	37-42	76-90
6	31-35	85-98	43-49	91-105
7	36-40	99-112	50-57	106-120

TABLE 9. Markov Chain cells/slice ranges.

*Bike*

*j*

	<b>0.9143</b>	0.0564	0.0160	0.0056	0.0028	0.0021	0.0021	0.0007
	0.2428	<b>0.5405</b>	0.1358	0.0462	0.0116	0.0116	0.0087...	0.0029
	0.0510	0.3214	<b>0.4082</b>	0.1480	0.0561	0.0051	0.0102	0
<i>i</i>	0.0915	0.0423	0.3028	<b>0.3944</b>	0.1197	0.0493	0	0
	0.1667	0.0500	0.0667	<b>0.3833</b>	0.2000	0.1167	0.1067	0
	0.1463	0.1220	0	0.1707	<b>0.2927</b>	0.1951	0.0488	0.0244
	0	0.0400	0	0.0400	0	0.4400	<b>0.4800</b>	0
	0	0	0	<b>0.5000</b>	0	0	<b>0.5000</b>	0

FIGURE 9. Markov Chain transition probability matrix for *Bike* video.

*Flowg*

*j*

	<b>0.8811</b>	0.1063	0.0107	0.0018	0	0	0	0
	0.1816	<b>0.6944</b>	0.1218	0.0021	0	0	0	0
	0	0.1296	<b>0.5556</b>	0.2840	0.0309	0	0	0
<i>i</i>	0.0168	0.0168	0.0252	<b>0.5294</b>	0.4118	0	0	0
	0.1583	0	0	0	0.0360	<b>0.4892</b>	0.3165	0
	0.0965	0.0088	0	0.0088	0.0965	<b>0.4912</b>	0.2982	0
	0.1228	0	0	0	0.0526	0.1228	<b>0.6316</b>	0.0407
	0	0	0	0	0	0	<b>0.5714</b>	0.4286

FIGURE 10. Markov Chain transition probability matrix for *Flowg* video.

*Tennis*

*j*

	<b>0.9023</b>	0.0635	0.0080	0.0066	0.0066	0.0058	0.0073	0
	<b>0.5342</b>	0.4064	0.0502	0.0046	0.0046	0	0	0
	0.0556	0.1587	<b>0.4603</b>	0.2778	0.0397	0.0079	0	0
<i>i</i>	0.0423	0.1217	0.1534	<b>0.3704</b>	0.2116	0.0899	0.0106	0
	0.0240	0	0.1040	0.3040	<b>0.4160</b>	0.1360	0.0160	0
	0	0	0.0292	0.2263	0.0730	<b>0.5182</b>	0.1533	0
	0	0	0	0.0649	0.1039	0.2338	<b>0.5325</b>	0.0649
	0	0	0	0	0	<b>0.8000</b>	0.2000	0

FIGURE 11. Markov Chain transition probabilities for *Tennis* video.



four pdf plots have roughly similar shapes. This would indicate that we might be able to use the Markov Chain to model a wide range of video sequences with a specific set of transition probabilities.

## 8.0 Conclusion

The compression ratio of the video sequences was greatly affected by its content. *Flowg* had the lowest compression ratio of the three video sequences. The distribution of macroblock type gave an indication as to why one video sequence had a better compression ratio than another. It was shown that a symmetrical dynamic bandwidth allocation scheme, where bandwidth is increased by one standard deviation, might not work well for video sequences containing B frames. This is due to the steep rise in the number of cells/slice as the sequence transitions from B to I or P frames. It was recommended that possibly a non-symmetrical approach, where bandwidth increases to the peak bandwidth and slowly decreases by one or more standard deviations, might be more appropriate.

The autocorrelation for the three video sequences was shown to be periodic and decayed with a linear negative slope. The period of the autocorrelation was equal to the interval between the start of an I or P picture and the beginning of the next I or P picture. The peak-to-mean ratio ranged from 6.2159 for *Bike* to 3.9462 for *Flowg*. This appears to show a proportional relationship between compression ratio and peak-to-mean ratio since *Bike* had the highest compression ratio.

As shown by the QQ plots, the Gamma pdf was found to fit the data well for *Bike*, but not for *Flowg* and *Tennis*. Significant deviations from linear in the QQ plots resulted from the gaps which existed between the Gamma pdf and the histogram data. The TSM *AllMux* sequence did appear to fit the Gamma distribution well. *AllMux* showed a reduction of the aggregate peak-to-mean ratio and coefficient-of-variation. A symmetrical dynamic bandwidth allocation scheme, where bandwidth increased/decreased by one standard deviation, would be feasible in this case.

It was indicated that basing traffic prediction for dynamic bandwidth allocation schemes from the video bit stream could lead to invalid requests for bandwidth. This was caused by the significant differences between the number of cells/frames for I/P frames and B frames. We proposed that the traffic predictor monitor only I frames. One drawback to this approach; however, is that the video stream might have to be parsed by the traffic predictor

in order to determine the frame type. It might be possible to avoid this by using a threshold and monitoring frames which only exceed this threshold.

An 8-state Markov Chain produced a pdf which fits the video data well. This indicated that the Markov Chain would be a good model for video sequences containing B frames. The Markov Chain also generated a pdf which fit the *AllMux* data well. Comparing the pdf for all three video sequences generated by the Markov Chain, we saw that they all had similar shapes. This indicated that it might be possible to model a variety of video sequences with a single Markov Chain.

Future work would involve studying a wider variety of VBR encoded video sequences to determine if they can be categorized into certain statistical classes. We would like to study longer video sequences to determine if the statistics still adhere to the results found in this paper and to generate a video sequence from the Markov Chain and determine if their autocorrelation functions fit the original data. We would also like to continue to explore dynamic bandwidth allocation and traffic prediction issues relating to I/B/P frame sequences. We would also like to develop a more sophisticated traffic prediction scheme which would handle I/B/P sequences. Finally, we would like to explore further the merits of TSM by attempting to create a model of it or through simulation.

## Acknowledgments

We would like to Andy C. Hung, from Stanford University, for providing the three video sequences as well as information on their encoding. We would also like to thank Brian Smith, from the University of California at Berkeley, for providing the *mpeg\_play* software decoder and information regarding the decoding of the MPEG files. Finally, we would like to thank Rex Dwyer for providing a mathematical solution which was used in this study.

## References:

- [1] M. Kawarasaki and B. Jabbari, "B-ISDN Architecture and Protocol," *IEEE J. Select. Areas Commun.*, vol. 9, no. 9, pp. 1405-1415, December 1991.
- [2] D.G. Morrison, "Variable Bit Rate Video Coding for Asynchronous Transfer Mode Networks," *Br. Telecom Technol. J. (UK)*, Vol. 8, No. 3, July 1990, pp 70-80.
- [3] W. Verbiest, L. Pinno, and B. Voeten, "The Impact of the ATM Concept on Video Coding," *IEEE J. Select. Areas Commun.*, vol.6, no. 9, pp. 1623-1632, December, 1988.
- [4] M. Sidi, et al., "Congestion Control Through Input Rate Regulation," in *Proc. IEEE GLOBE-COM '89*, pp 49.3.1-49.3.5.

- [5] M. Ghanbari, "Two-layer Coding of Video Signals for VBR Networks," *IEEE J-SAC*, Vol. 7, No. 5, pp771-781, June 1989.
- [6] M. Ghanbari and V. Seferidis, "Cell-Loss Concealment in ATM Video Codecs," *IEEE Trans. Cir. Sys. Video Tech.*, Vol. 3, No. 3, June 1993, pp 238-247.
- [7] F. Kishino, K. Manabe, Y. Hayashi, and H. Yasuda, "VBR Coding of Video Signals for ATM Networks," *IEEE J. Select. Areas Commun.*, vol. 7, no. 5, pp. 801-806, June 1989.
- [8] P. Boyer, "A Congestion Control for the ATM," *ITC Seventh Specialist Seminar*, October 1990.
- [9] P. Pancha and M. El Zarki, "Bandwidth-allocation Schemes for Variable-Bit-Rate MPEG Sources in ATM Networks," *IEEE Trans. on Circuits and Systems for Video Tech.*, vol. 3, no. 3, pp 190-198, June 1993.
- [10] H. Heeke, "A Traffic-Control Algorithm for ATM Networks," *IEEE Trans. on Circuits and Systems for Video Tech.*, vol. 3, no. 3, pp 182-189, June 1993.
- [11] Motion Pictures Expert Group, "Coding of Moving Pictures and Associated Audio for Digital Storage Media at up to about 1.5 Mbits/sec," ISO 2-11172 rev. Part 2: Video, November 22, 1991.
- [12] D. Le Gall, "MPEG: A Video Compression Standard for Multimedia Applications," *Commun. of the ACM*, vol. 34, no. 4, pp 47-58, April 1991.
- [13] M. Nomura, T. Fujii, and N. Ohta, "Basic Characteristics of Variable Rate Video Coding in ATM Environment," *IEEE J. Select. Areas Commun.*, vol. 7, no. 5, pp. 752-760, June 1989.
- [14] J. Zdepski, K. Joseph, and D. Raychaudhuri, "Packet Transport of VBR InterPicture DCT Compressed Digital Video on a CSMA/CD LAN," *GLOBECOM 1989*, pp. 886-890.
- [15] R. Grunenfelder, J. Cosmas, S. Manthorpe, and A. Odinma-Okafor, "Characterization of Video Codecs as AutoRegressive Moving Average Processes and Related Queueing System Performance," *IEEE J. Select. Areas Commun.*, vol. 9, no. 3, pp. 284-293, April 1991.
- [16] B. Jabbari, F. Yegenoglu, Y. Kuo, S. Zafar, and Y. Q. Zhang, "Statistical Characterization and Block-Based Modeling of Motion-Adaptive Coded Video," *IEEE Trans. on Circuits and Systems for Video Tech.*, vol. 3, no. 3, pp 199-207, June 1993.
- [17] A.W. Bragg and W. Chou, "Analytic Models and Characteristics of Video Traffic in High Speed Networks," *Proc. of the 2nd Intl. Workshop MASCOTS '94*, pp. 68-73.
- [18] B. Maglaris, D. Anastassiou, P. Sen, G. Karlsson, and J. Robbins, "Performance models of statistical multiplexing in packet video communications," *IEEE Trans. Commun.*, vol. 36, no. 7, pp. 834-844, July 1988.
- [19] S. Huang, "Modeling and Analysis for Packet Video," *GLOBECOM 1989*, pp 881-885.
- [20] Y. Yasuda, H. Yasuda, N. Ohta, and F. Kishino, "Packet Video Transmission through ATM Networks," *GLOBECOM 1989*, pp. 876-880.
- [21] P. Sen, B. Maglaris, N. E. Rikli, and D. Anastassiou, "Models for Packet Switching of Variable-Bit-Rate Video Sources," *IEEE J. Select. Areas Commun.*, vol. 7, no. 5, pp. 865-869, June 1989.
- [22] D. Heyman, A. Tabatabai, and T. V. Lakshman, "Statistical Analysis and Simulation Study of Video Teleconference Traffic in ATM Networks," *IEEE J. Select. Areas Commun.*, vol. 2, no. 1, pp. 49-59, March 1992.
- [23] P. Skelly, M. Schwartz and Sudhir Dixit, "A Histogram-Based Model for Video Traffic Behaviour in an ATM Multiplexer," *IEEE/ACM Transactions on Networking*, Vol. 1, No. 4, pp. 446-459, August 1993.

- [24] F. Yegenoglu, B. Jabbari, Y. Q. Zhang, "Motion-Classified Autoregressive Modeling of Variable Bit Rate Video," *IEEE Trans. on Circuits and Systems for Video Tech.*, vol. 3, no. 1, pp 42-53, February 1993.
- [25] B. Melamed and B. Sengupta, "TES Modeling of Video Traffic," *IEICE Trans. Commun.*, vol. E75-B, no. 12, pp 1292-1300, December 1992.
- [26] R. M. Rodriguez-Dagnino, M. Khansari, and A. Leon-Garcia, "Prediction of Bit Rate Sequences of Encoded Video Signals," *IEEE J. Select. Areas Commun.*, vol. 9, no. 3, pp. 305-314, April 1991.
- [27] M. Livny, B. Melamed, and A. K. Tsiolis, "The Impact of AutoCorrelation on Queuing Systems," *Management Science*, vol. 39, no. 3, pp. 322-339, March 1993.
- [28] P. Pancha and M. El Zarki, "A Look at the MPEG Video Coding Standard for Variable Bit Rate Video Transmission," *INFOCOM '92*, pp 85-94.
- [29] R. Kishimoto, Y. Ogata, and F. Inumaru, "Generation Interval Distribution Characteristics of Packetized Variable Rate Video Coding Data Streams in an ATM Network," *IEEE J. Select. Areas Commun.*, vol. 7, no. 5, pp. 833-841, June 1989.
- [30] Mendenhall, Scheaffer and Wackerly, *Mathematical Statistics with Applications*, 2nd edition, Duxbury Press, 1981.
- [31] R. Gnanadesiran, *Methods for Statistical Data Analysis of Multivariate Observations*, John Wiley & Sons, 1977.

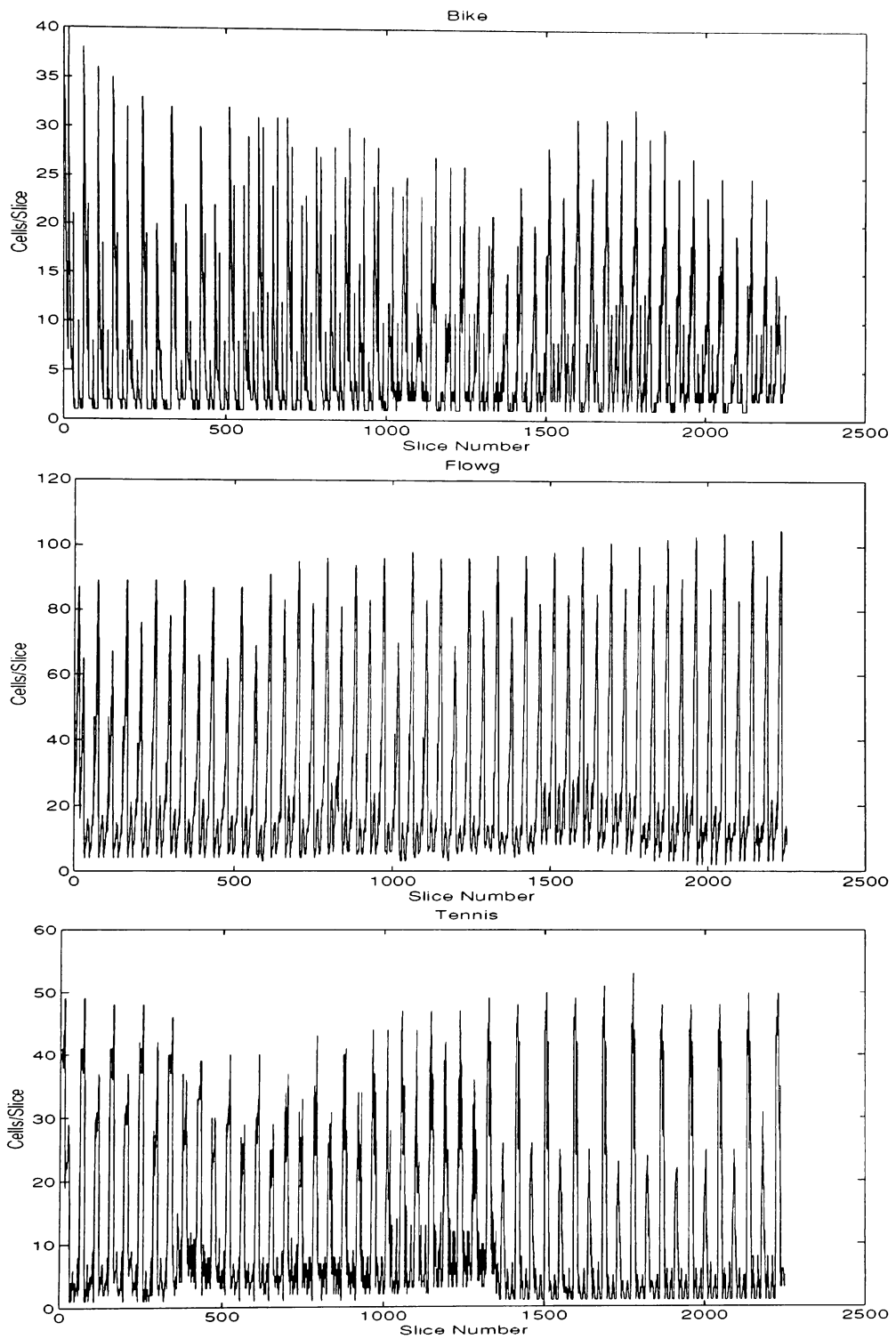


**FIGURE 14.** Cells/slice plot of 2250 slices (150 pictures) from *Bike*, *Flowg* and *Tennis*

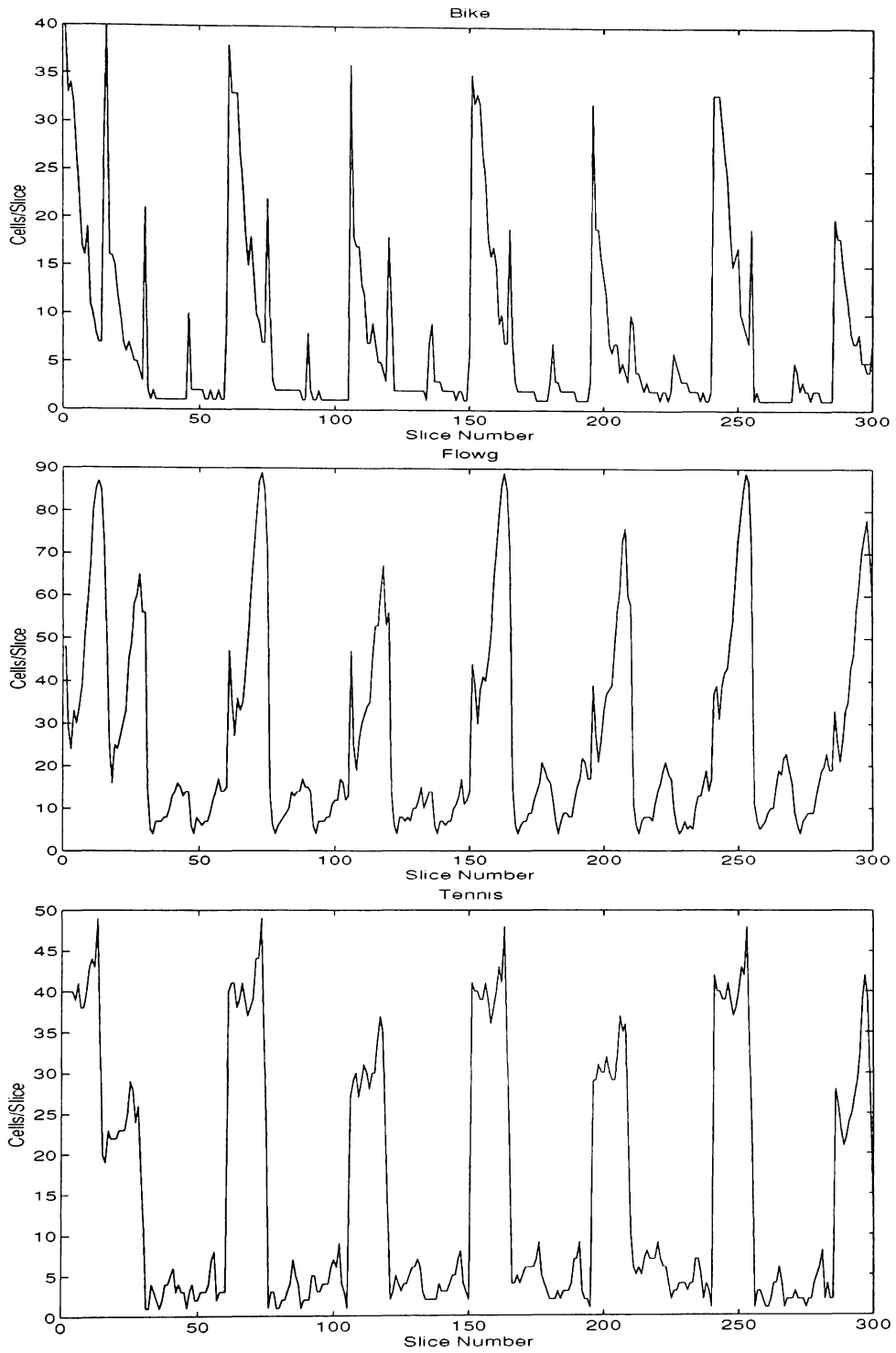


**FIGURE 15.** Cells/slice plot of first 300 slices from *Bike*, *Flowg* and *Tennis*.

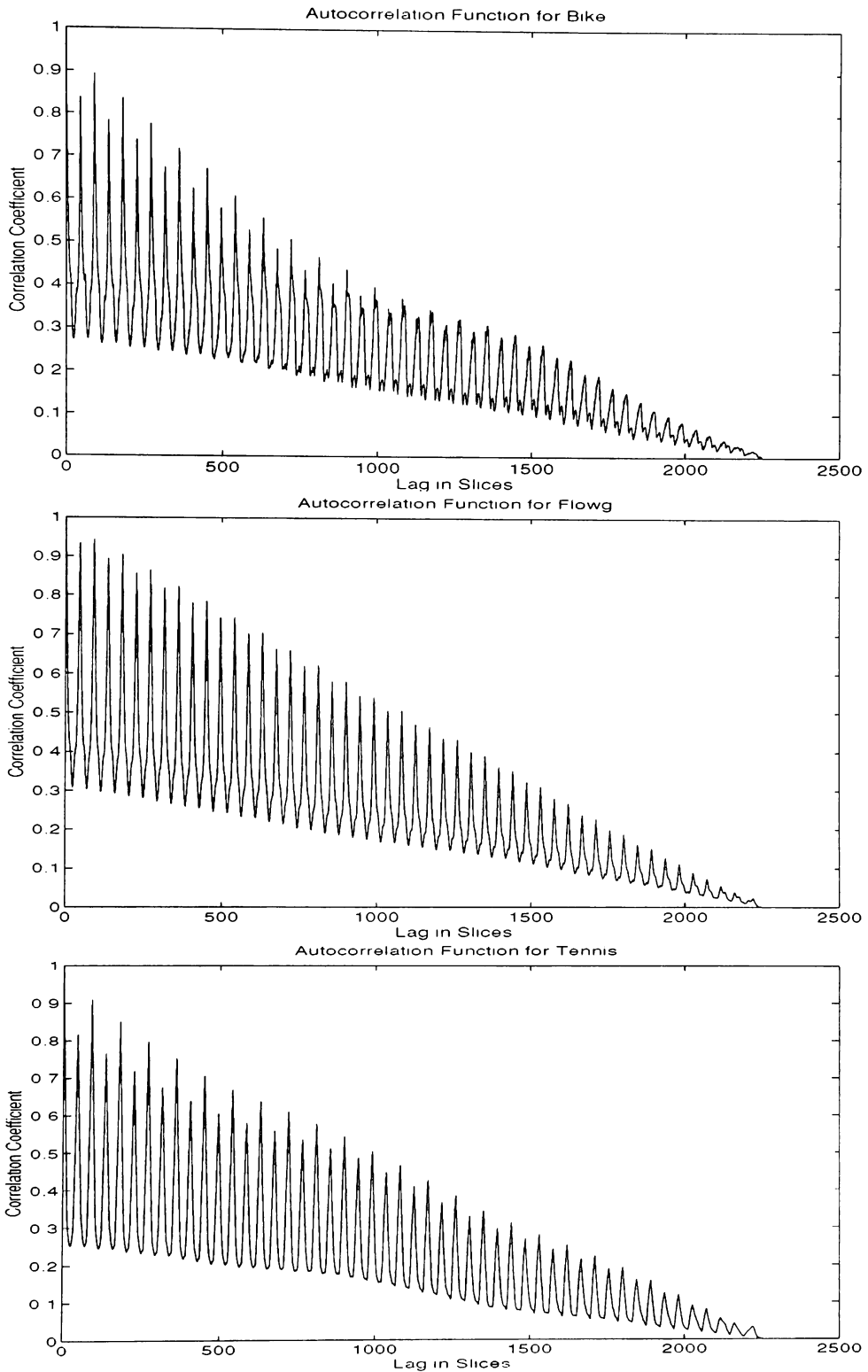


**FIGURE 16. Autocorrelation function for *Bike*, *Flowg* and *Tennis***

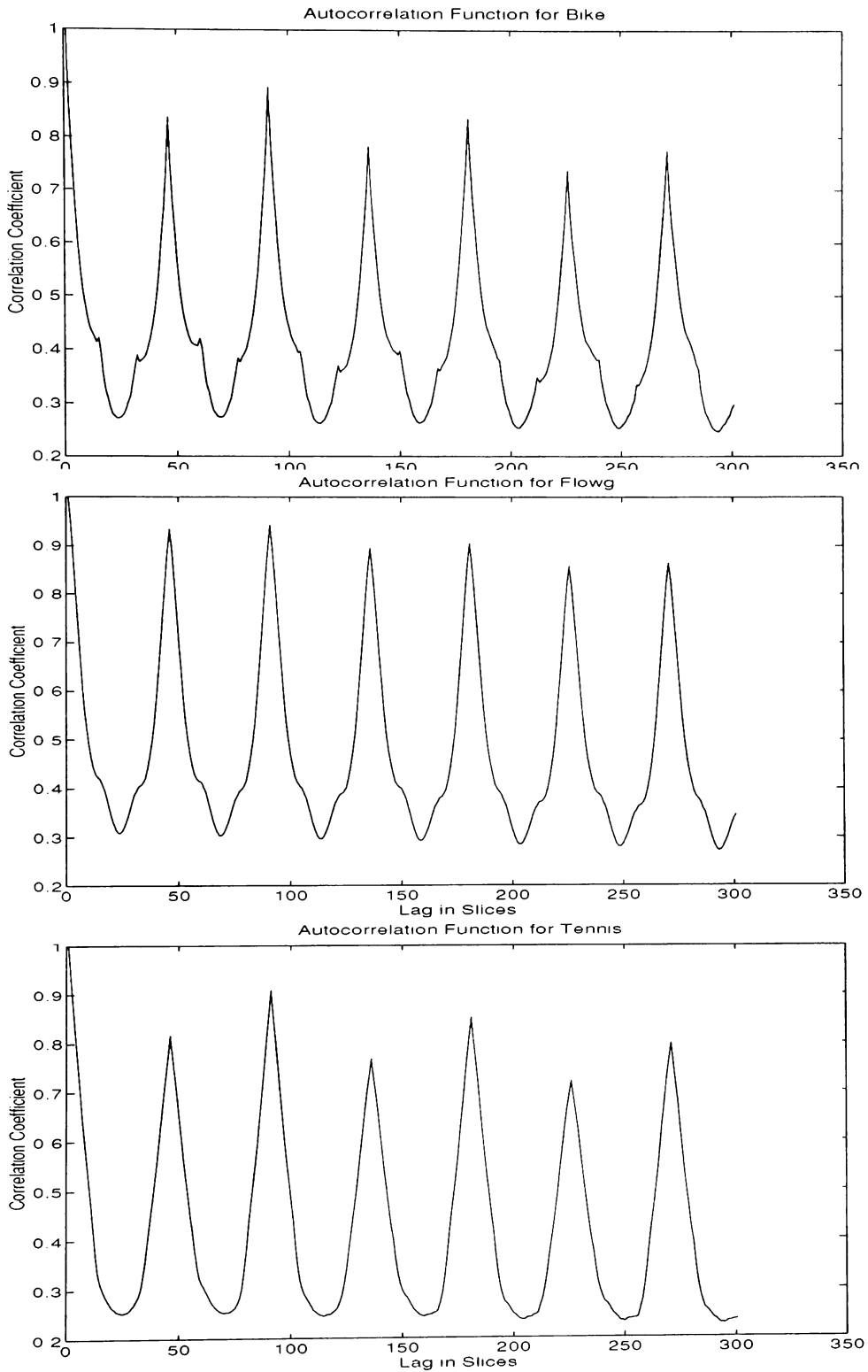


**FIGURE 17. Autocorrelation Function for 300 slices of *Bike*, *Flowg* and *Tennis*.**

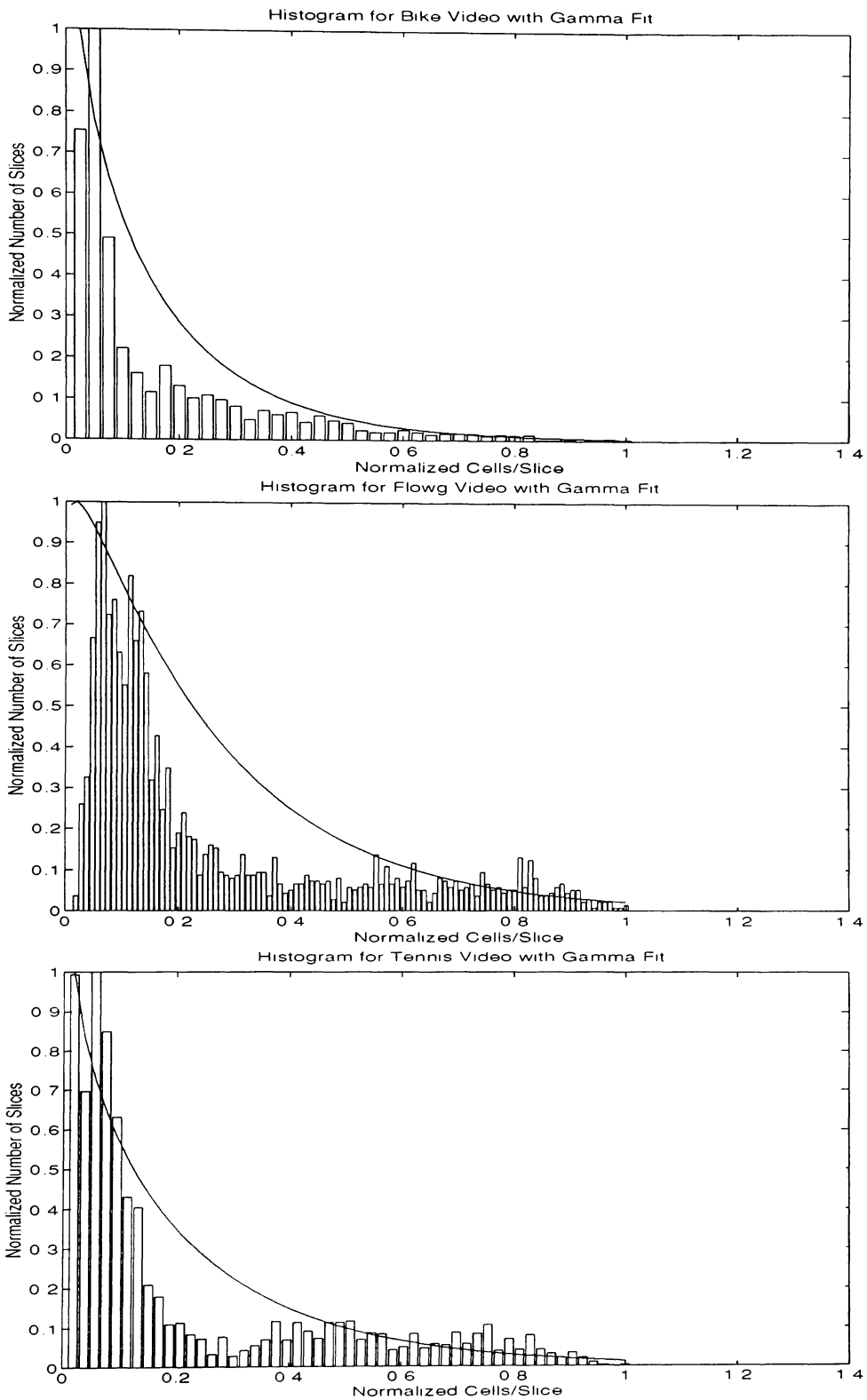


FIGURE 18. Cells/slice histograms of *Bike*, *Flow* and *Tennis*.

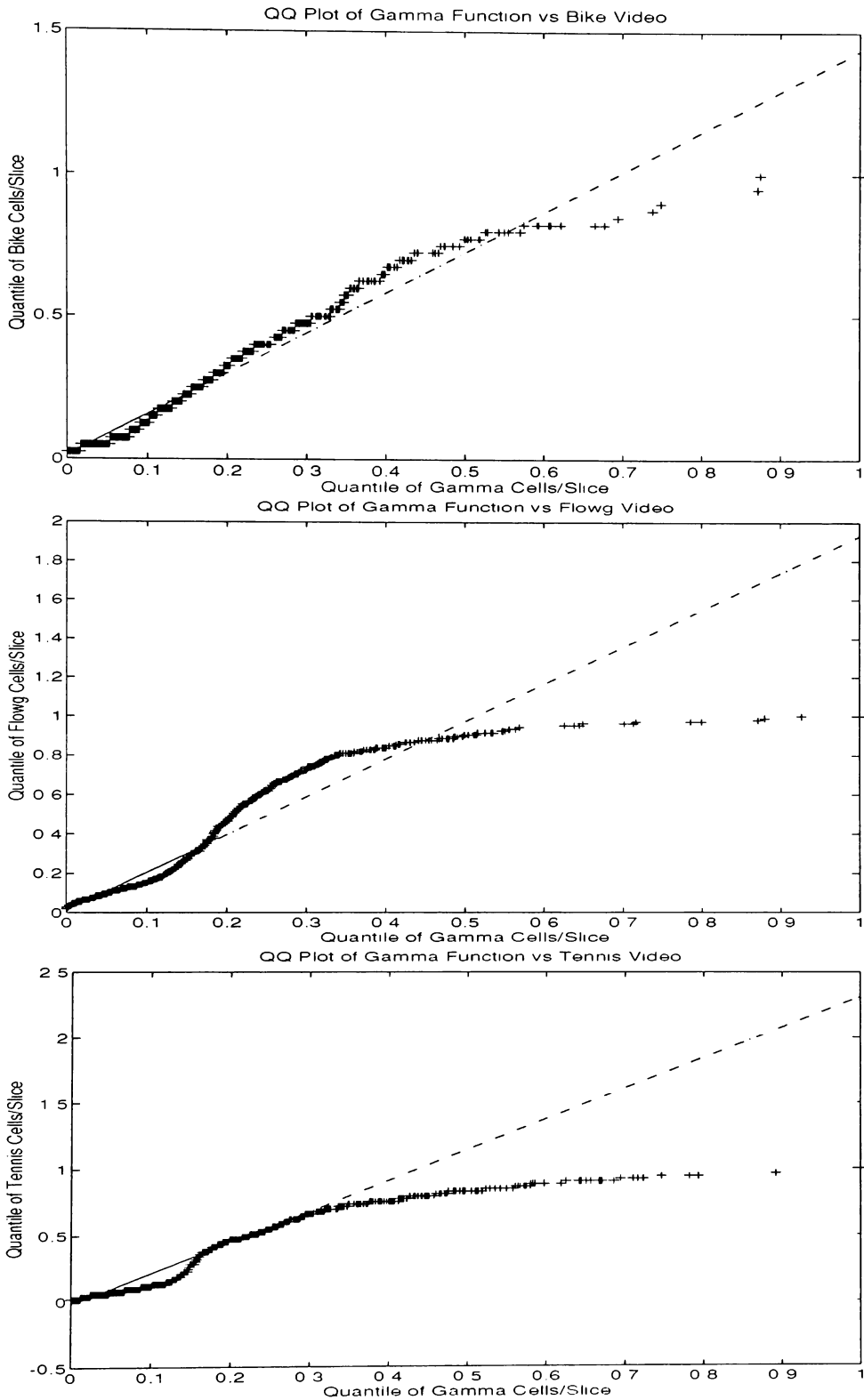
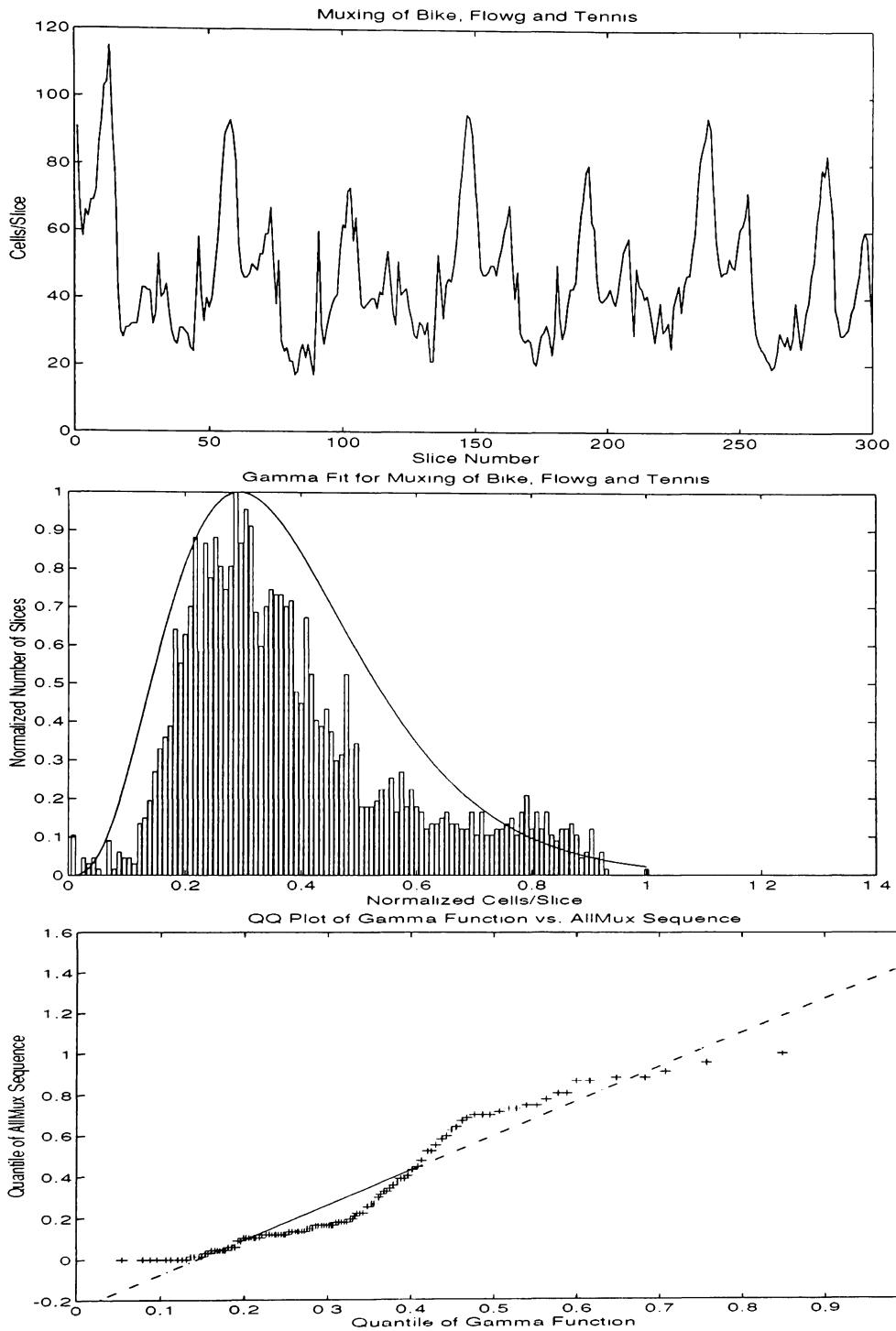


FIGURE 20. QQ plots of *Bike*, *Flowg* and *Tennis* vs Gamma distribution.



**FIGURE 21.** Histogram and QQ plot of combined *Bike, Flowg, Tennis* Cells/slice and gamma pdf overlay.

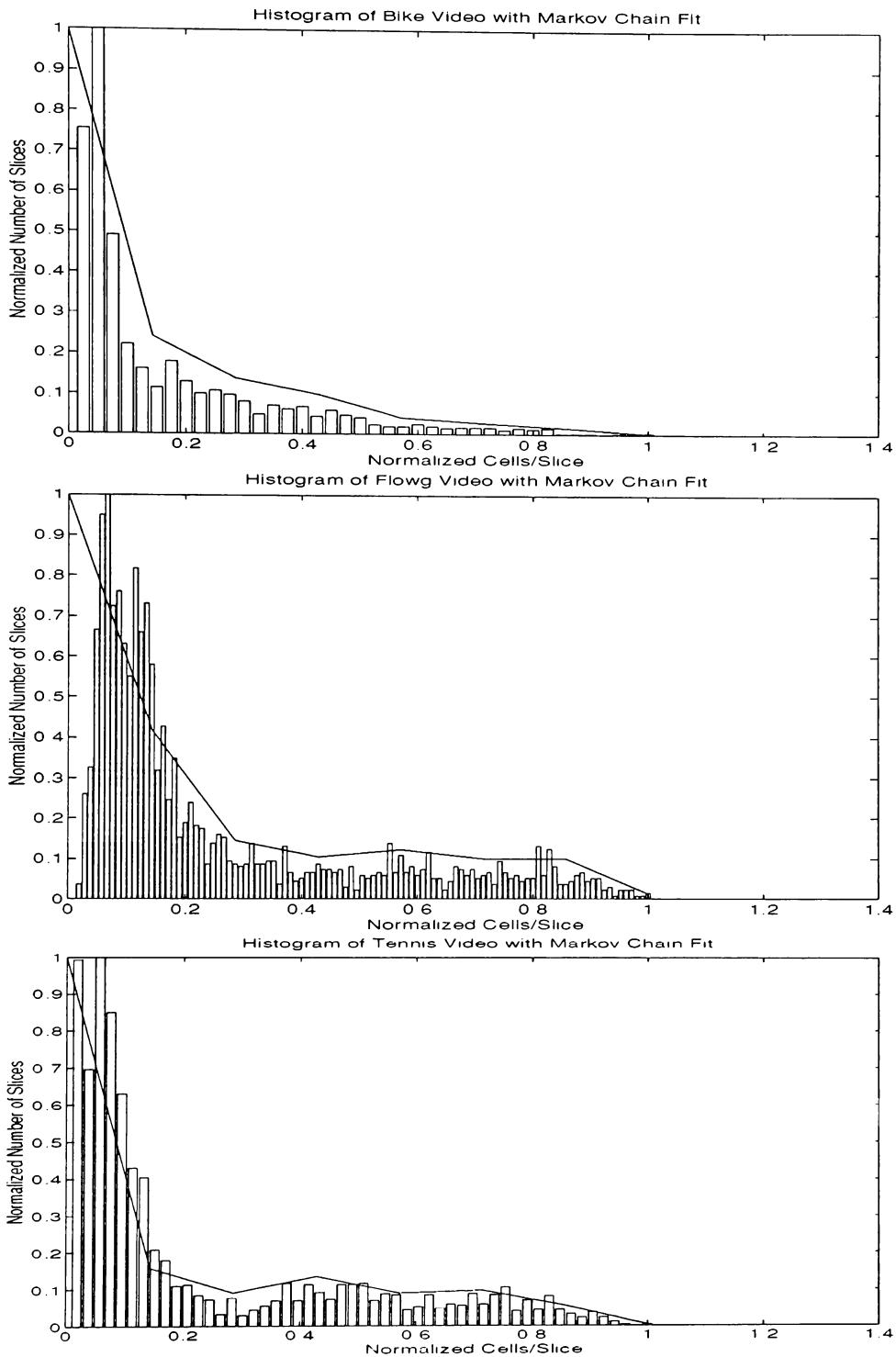


FIGURE 22. 8-state Markov Chain pdf fit of cells/slice data

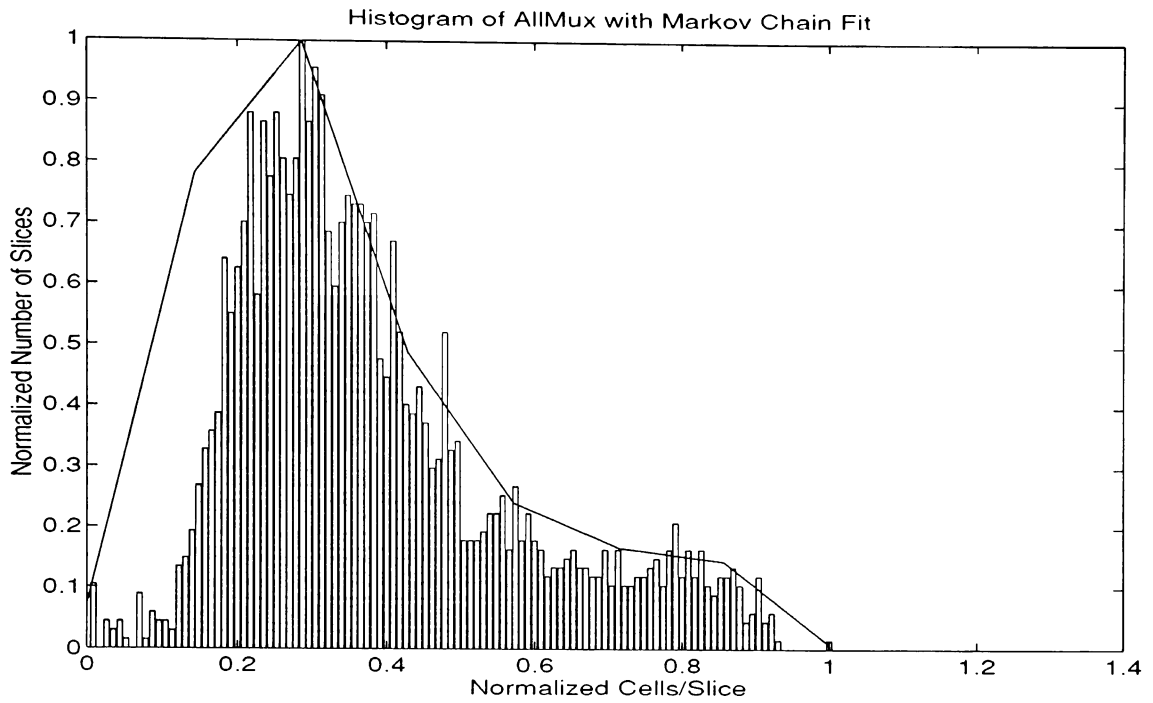


FIGURE 23. Histogram of AllMux with 8-state Markov chain Fit

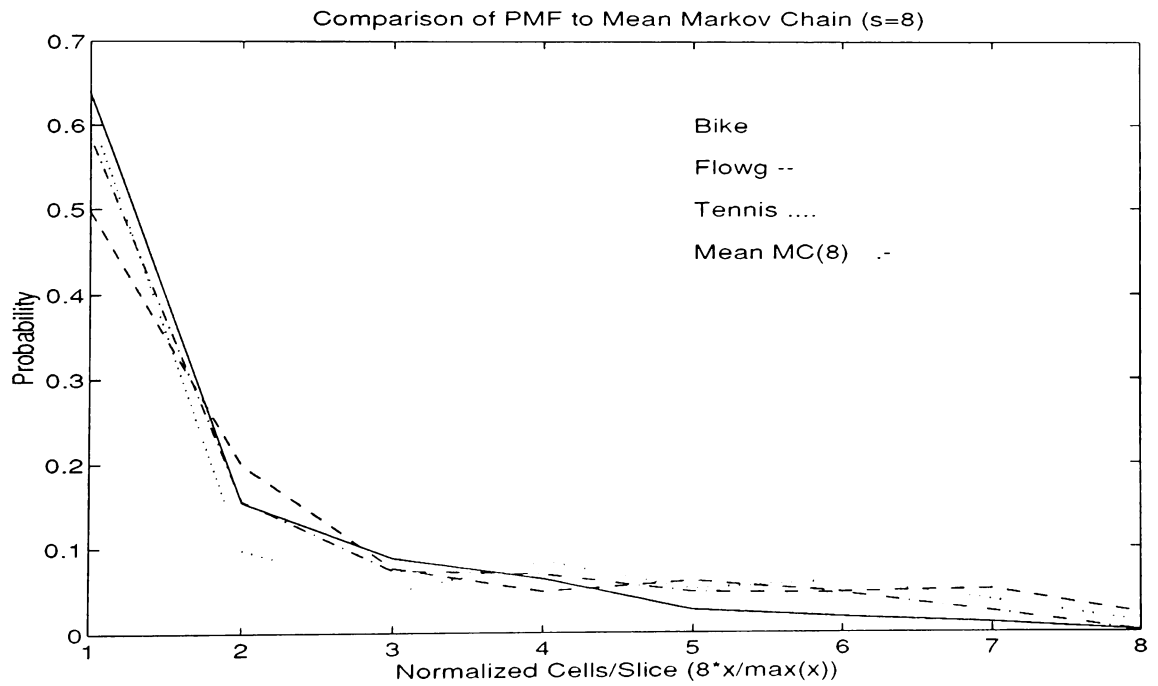


FIGURE 25. Comparison of Markov Chain steady-state distributions of all three video sequences and Mean Markov Chain.